Exhumation kinematics of the Cycladic Blueschists unit and back-arc extension, insight from the Southern Cyclades (Sikinos and Folegandros Islands, Greece)

Romain Augier, Laurent Jolivet, Leslie Gadenne, Abdeltif Lahfid, Olivier Driussi

AGU PUBLICATIONS

Tectonics

RESEARCH ARTICLE
10.1002/2014TC003664

Key Points:
- Deformation presents a marked top-to-the-north asymmetry
- The South Cycladic thrust is strongly reworked by top-to-the-north movements
- Deformation thus appears genuinely asymmetric in the center of the Aegean domain

Supporting Information:
- Readme
- Text S1
- Text S2
- Figure S1

Correspondence to:
R. Augier,
romain.augier@univ-orleans.fr

Citation:
Augier, R., L. Jolivet, L. Gadenne, A. Lahfid, and O. Driussi (2015), Exhumation kinematics of the Cycladic Blueschists unit and back-arc extension, insight from the Southern Cyclades (Sikinos and Folegandros Islands, Greece), *Tectonics*, *34*, doi:10.1002/2014TC003664.

Received 24 JUN 2014
Accepted 19 DEC 2014
Accepted article online 29 DEC 2014

Exhumation kinematics of the Cycladic Blueschists unit and back-arc extension, insight from the Southern Cyclades (Sikinos and Folegandros Islands, Greece)

Romain Augier[1,2,3], Laurent Jolivet[1,2,3], Leslie Gadenne[1,2,3], Abdeltif Lahfid[3], and Olivier Driussi[1,2,3,4]

[1]Université d'Orléans, ISTO, UMR 7327, Orléans, France, [2]CNRS/INSU, ISTO, UMR 7327, Orléans, France, [3]BRGM, ISTO, UMR 7327, Orléans, France, [4]Now at Université de Toulouse, CNRS-IRD, Géosciences Environnement Toulouse, Observatoire Midi Pyrénées, Toulouse, France

Abstract Current models for the Oligo-Miocene postorogenic back-arc extension of the Aegean domain suggest that stretching is accommodated by two bivergent detachment systems of opposing shear sense. The coexistence in the Eocene of a top-to-the-south thrust at the base of the Cycladic Blueschists unit and top-to-the-north extensional shear zones at the roof raises the problem of differentiating synorogenic and postorogenic deformations with similar directions and shear senses. Based on structural field data, this study shows that the postorogenic deformation recorded in the Southern Cyclades is extremely asymmetric as the Cycladic Blueschists unit is pervasively affected by top-to-the-north shearing deformation distributed on four main shear zones. All activated in greenschist-facies conditions, some of these shear zones operated in the brittle regime during the final part of the exhumation. The Cycladic Blueschists/Cycladic Basement contact displays clear polyphased deformation with the preservation of top-to-the-south thrust kinematics. Thermal structure of the Cycladic Blueschists unit with regard to position of ductile shear zones was retrieved using the Raman Spectroscopy of Carbonaceous Material peak-metamorphic temperatures. This study shows a series of major metamorphic gaps accommodating an upward and stepwise decrease of more than 200°C within the Cycladic Blueschists unit. Pressure-temperature estimates show that only lower parts of the Cycladic Blueschists unit recorded approximately 18–20 kbar for 530°C peak conditions. While flanking the West Cycladic Detachment System, which shows a top-to-the-south shear sense, the Southern Cyclades are dominated by a top-to-the-north noncoaxial shearing. Deformation is therefore genuinely asymmetric in the center of the Aegean domain.

1. Introduction

Whether crustal thinning in back-arc regions is mostly symmetrical (pure shear) or asymmetrical (simple shear) at large scale is key to understanding if lithospheric deformation is coupled or not to asthenospheric flow [*Jolivet et al.*, 2008; *Sternai et al.*, 2014]. In the Mediterranean realm, the retreat of the African slab triggered the formation of back-arc basins settled on collapsed portions of previously thickened continental lithosphere [e.g., *Dewey*, 1988; *Jolivet and Faccenna*, 2000; *Rosendaum et al.*, 2002]. This evolution resulted in the formation of the Alboran Sea, the Tyrrhenian Sea, the Pannonian Basin, and the Aegean Sea surrounded by series of arcuate orogenic belts whose kinematics is the consequence of the retreat dynamics rather than of the convergence of Africa and Eurasia at the boundaries of the deforming system [*Le Pichon and Angelier*, 1981; *Le Pichon*, 1982; *Malinverno and Ryan*, 1986; *Dewey*, 1988; *Platt and Vissers*, 1989; *Royden*, 1993; *Wortel and Spakman*, 2000; *Faccenna et al.*, 2004, 2007; *Spakman and Wortel*, 2004; *Jolivet et al.*, 2008]. Extensional tectonics within the back-arc domains induced a strong stretching at crustal scale and the formation of localized shallow-dipping detachments that contributed to the exhumation of Metamorphic Core Complexes (MCCs) [i.e., *Lister et al.*, 1984; *Urai et al.*, 1990; *Gautier and Brun*, 1994a; *Jolivet et al.*, 2004]. The internal kinematics of these MCCs as well as that of detachments shows consistent orientations and sense of shear over large regions. For example, in the Tyrrhenian Sea, the extensional kinematics is dominantly characterized by a top-to-the-east sense of shear [*Jolivet et al.*, 1998; *Rossetti et al.*, 1999; *Jolivet et al.*, 2008], while thrusts display both top-to-the-east and top-to-the-west kinematics. Similarly, in the Alboran domain, late exhumation stages controlled by westward slab retreat show a single top-to-the-west detachment

system [*García-Dueñas et al*., 1992; *Jabaloy et al*., 1993; *Martínez-Martínez et al*., 2004; *Jolivet et al*., 2004; *Augier et al*., 2005a, 2013]. In these cases, the general sense of shear toward the trench might be explained by the interactions between the subducting slab and the mantle that primarily control the basal drag below the upper plate [*Jolivet et al*., 2008; *Sternai et al*., 2014]. In the Aegean domain, kinematics of postorogenic extension is still a matter of debate, particularly since the last few years [e.g., *Huet et al*., 2009; *Jolivet et al*., 2010; *Ring et al*., 2011; *Grasemann et al*., 2012]. Top-to-the-north kinematics was first described in the center of the Cyclades in the footwall of the north dipping Naxos-Paros detachment (i.e., in the Naxos-Paros MCC) [e.g., *Urai et al*., 1990; *Buick*, 1991; *Gautier et al*., 1993]. More recently, it has also been suggested that the set of top-to-the-north detachments described in the northern part of the Cyclades link up to form the crustal-scale North Cycladic Detachment System (NCDS) [*Jolivet et al*., 2010] emphasizing a strong structural asymmetry of the back-arc domain. However, consistent top-to-the-SW kinematics was also described in the western part of the Cyclades [*Grasemann and Petrakakis*, 2007; *Tschegg and Grasemann*, 2009; *Iglseder et al*., 2011]. Sharing similar tectonometamorphic histories leading to the exhumation of the Cycladic Blueschists unit, these detachments were recently mechanically linked into a single major detachment system known as the South Cycladic Detachment System [*Ring et al*., 2011] or as the West Cycladic Detachment System [*Grasemann et al*., 2012] depending on the lateral extent of the regional correlation. The overall picture of the extensional kinematics of the whole domain appears, at first sight, marked by a more symmetrical deformation than previously thought [*Jolivet et al*., 1994] characterized by several detachment systems exhibiting opposed shear sense [*Grasemann et al*., 2012]. The picture is further complicated by the persistence of Eocene preextension orogenic in a broad sense structures often with the same direction and sense of shear as extension-related ones [*Gautier and Brun*, 1994a, 1994b; *Huet et al*., 2009; *Ring et al*., 2011]. It appears therefore crucial to clarify the distribution of kinematic indicators in the Aegean Sea and to unambiguously separate deformation related to orogenic and postorogenic stages.

The Southern Cyclades are exemplary of this debate [*Lister et al*., 1984; *Huet et al*., 2009; *Ring et al*., 2011]. Most of the data existing in this region were acquired on Ios Island [e.g., *Lister et al*., 1984; *Vandenberg and Lister*, 1996; *Huet et al*., 2009; *Ring et al*., 2011] and farther west, on Serifos [e.g., *Tschegg and Grasemann*, 2009; *Iglseder et al*., 2009; *Grasemann et al*., 2012]. Located only at a few kilometers from Ios and presenting at first glance the same strategic interest, Sikinos and Folegandros Islands have been left mostly unexplored apart from the Greek Institute of Geology and Mineral Exploration (G-IGME; the Geological survey of Greece) geological maps [*Avdis and Photiades*, 1999] and a few other studies [e.g., *Sowa*, 1985; *Gupta and Bickle*, 2004]. The easternmost evidence of the West Cycladic Detachment System (WCDS) has been described on Serifos (Figure 1) [*Grasemann et al*., 2012]. Top-to-the-south kinematics has been described in Sifnos [*Ring et al*., 2011], while top-to-the-north extensional kinematics has been reported from the Northern and Central Cyclades including Ios [*Huet et al*., 2009]. Sikinos and Folegandros are just located in the intervening zone where no clear kinematics has yet been described, apart from some indications of top-to-the-north [*Gautier and Brun*, 1994b] and of top-to-the-south shear senses [*Ring et al*., 2011]. This paper presents an integrated study of these two islands that complete the regional scheme of kinematic indicators and shed light on the relations between top north and top south kinematics indicators.

2. Geological Setting

2.1. The Cycladic Archipelago

The Cycladic Archipelago (eastern Aegean Sea) corresponds to the foundering of the Hellenides-Taurides belt, formed by stacking of upper crustal units within a SW verging accretionary wedge as the result of the convergence between Apulian and European plates in the eastern Mediterranean (Figure 1) [e.g., *Aubouin and Dercourt*, 1965; *Brunn et al*., 1976; *Jacobshagen et al*., 1978]. Postorogenic extension of the Hellenic thickened crust started some 30–35 Ma ago by a combination of gravitational collapse and back-arc extension in a context of the southward retreat of the African slab [*Jolivet and Faccenna*, 2000; *Jolivet and Brun*, 2010]. Despite a strong overprint of the orogenic architecture during postorogenic extension, the original vertical superposition of nappe stack is often preserved at the scale of the whole Aegean domain [e.g., *Bonneau*, 1984; *Jacobshagen*, 1986; *Jolivet et al*., 2004; *van Hinsbergen et al*., 2005; *Ring et al*., 2010]. In the Cycladic Archipelago, three main tectonometamorphic units are classically recognized: the upper Cycladic unit, the intermediate Cycladic Blueschists unit, and the lowermost Cycladic Basement unit.

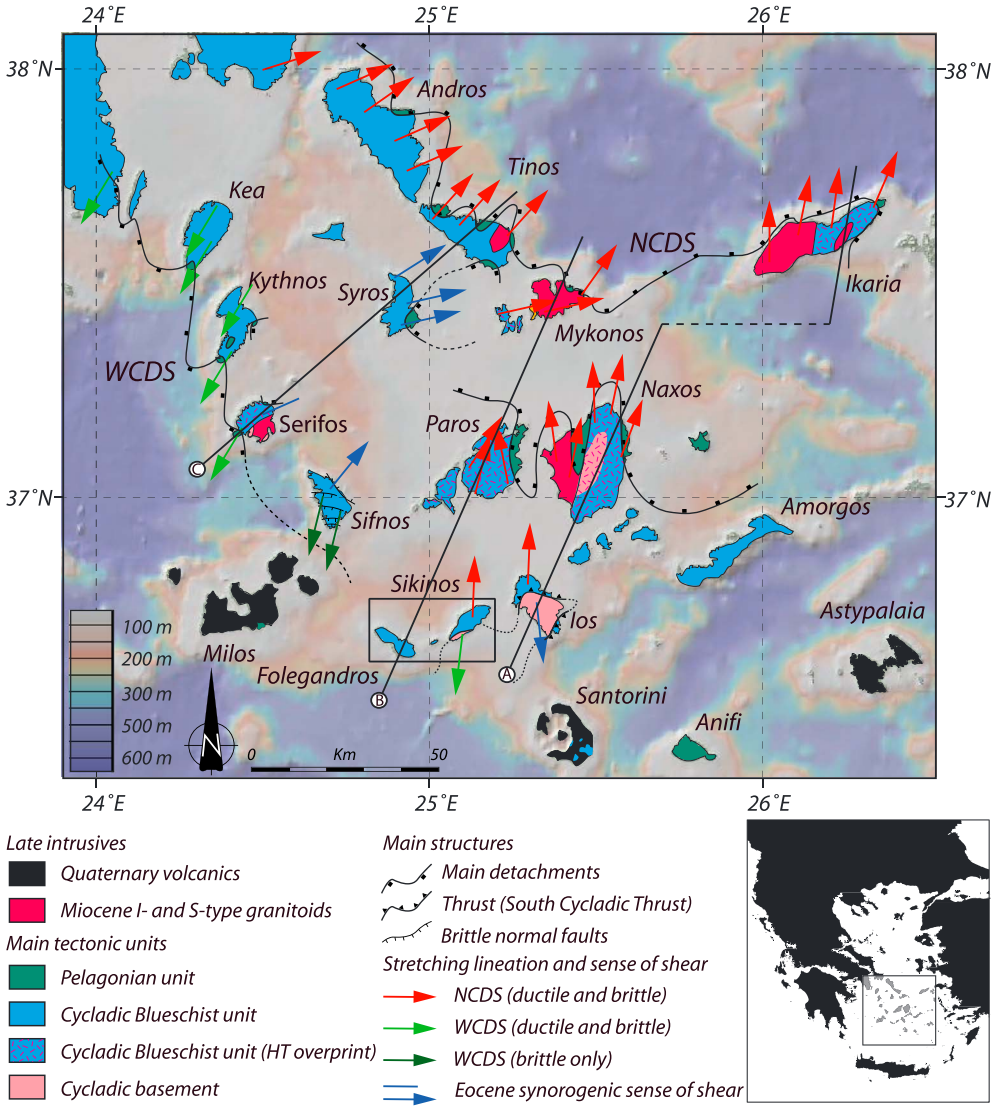

Figure 1. Geological map of the studied area. Tectonic map of both synorogenic and postorogenic structures in the Cycladic archipelago, modified after *Jolivet et al.* [2004]. Arrows indicate the ductile sense of shear associated to the Eocene episode during which the Cycladic Blueschists and the Cycladic Basement were buried and partly exhumed in a subduction context [*Trotet et al.*, 2001a, 2001b; *Huet et al.*, 2009] and to the Oligo-Miocene extensional episode [*Lister et al.*, 1984; *Faure et al.*, 1991; *Gautier and Brun*, 1994a; *Vandenberg and Lister*, 1996; *Forster and Lister*, 1999a; *Jolivet and Patriat*, 1999; *Mehl et al.*, 2005, 2007; *Huet et al.*, 2009; *Jolivet et al.*, 2010; *Ring et al.*, 2011; *Grasemann et al.*, 2012]. Indicated is the location of the cross sections presented in Figure 13.

The upper Cycladic unit corresponds to the Upper Cycladic Nappe [*Jolivet et al.*, 2004], a lateral equivalent of the Pelagonian nappe [e.g., *Bonneau*, 1984; *Jolivet et al.*, 2004] that is found in continental Greece, most of the Cycladic Archipelago, and all the way to Crete at the top of the Hellenic orogenic structure (Figure 1) [e.g., *Reinecke et al.*, 1982; *Bonneau*, 1984; *Papanikolaou*, 1987]. In the Cyclades, it generally crops out as isolated klippens, essentially made of ophiolitic material (i.e., serpentinites, gabbros, and basalts) such as in Andros, Tinos, or Mykonos in the Northern Cyclades or as in Kea, Kythnos, and Serifos in the Western Cyclades [e.g., *Jolivet et al.*, 2010; *Grasemann et al.*, 2012]. On other islands, as Syros or Donoussa, the Pelagonian nappe consists in continental gneisses yielding Late Cretaceous ages [*Jansen*, 1977; *Dürr et al.*, 1978; *Maluski et al.*, 1987; *Patzak et al.*, 1994; *Katzir et al.*, 1996]. Detrital shallow marine and continental sediments locally form the uppermost unit on Mykonos, Ikaria, Paros, and Naxos [e.g., *Angelier et al.*, 1978; *Sánchez-Gómez et al.*, 2002; *Kuhlemann et al.*, 2004]. Conglomerates mostly contain pebbles issued from the Upper Cycladic Nappe and reworked volcanic rocks and granites as young as 10 Ma [e.g., *Sánchez-Gómez et al.*, 2002], but clasts

issued from the Cycladic Blueschists are not reported. Importantly, the activity of the detachment is also constrained by syntectonic deposition of sediments over the upper Cycladic unit [*Kuhlemann et al*., 2004; *Lecomte et al*., 2010].

The Cycladic Blueschists unit crops out in most of the Cyclades as a composite unit including a significant component of metabasic rocks interleaved with metapelites and marbles, all conspicuously equilibrated in blueschist-facies conditions [e.g., *Blake et al*., 1981; *Bonneau*, 1984; *Avigad and Garfunkel*, 1991; *Keiter et al*., 2004]. Metabasites, mainly derived from mid-ocean ridge basalt-type basalts [*Schliestedt et al*., 1987; *Bröcker*, 1990] correspond to ancient flows, tuffs, blocks in metaconglomerate layers, or even large-scale mafic olistostrome as exposed on Syros [*Bonneau et al*., 1980; *Keiter et al*., 2004]. Considered as a Triassic to Late Cretaceous passive-margin sequence accompanied by transitional oceanic remnants, this unit is generally interpreted as a lateral equivalent of the Pindos oceanic zone in the Hellenides edifice [e.g., *Bonneau*, 1984; *Bröcker and Pidgeon*, 2007]. The Cycladic Blueschists unit experienced a complex alpine tectonometamorphic evolution, with an early burial in high pressure/low temperature (HP-LT) conditions reaching blueschists to eclogite-facies conditions during the Eocene followed by a greenschist to amphibolite overprint of variable intensity during the Oligocene and the Miocene (Figure 1) [*Altherr et al*., 1979, 1982; *Wijbrans and McDougall*, 1986; *Buick*, 1991; *Keay et al*., 2001; *Duchêne et al*., 2006].

The Cycladic Basement unit crops out in the central and Southern Cyclades (i.e., on Naxos, Paros, Sikinos, and Ios, Figure 1) [e.g., *Andriessen et al*., 1987]. This unit is composed of Variscan granitoid mantled by micaschists that retain either metamorphic relics of amphibolite-facies assemblages and radiometric ages suggesting a complex prealpine history [e.g., *Henjes-Kunst and Kreuzer*, 1982; *Andriessen et al*., 1987; *Keay*, 1998; *Photiades and Keay*, 2003]. The Cycladic Basement unit is classically considered as a part of the Apulian southern margin of the Pindos basin [e.g., *Bonneau and Kienast*, 1982; *Keay and Lister*, 2002]. Just as the Cycladic Blueschists unit, the Cycladic Basement unit shows a complex alpine tectonometamorphic evolution, with an initial, subduction-related burial in HP-LT conditions during the Eocene whose trace has been obscured by an Oligo-Miocene high-temperature (HT) local overprint (Figure 1) [*van der Maar*, 1980; *van der Maar and Jansen*, 1983; *Vandenberg and Lister*, 1996; *Baldwin and Lister*, 1998; *Gupta and Bickle*, 2004; *Huet*, 2010]. On Naxos and Paros, both the Cycladic Basement and the base of the Cycladic Blueschists units thus experienced a partial-melting stage in amphibolite to granulite-facies conditions [i.e., *Jansen and Schuiling*, 1976; *Buick*, 1988; *Buick and Holland*, 1989; *Katzir et al*., 1999; *Vanderhaeghe*, 2004; *Duchêne et al*., 2006]. In the Southern Cyclades, although based on limited mineralogical occurrences, an initial HP-LT imprint remains still observable [*van der Maar et al*., 1981; *van der Maar and Jansen*, 1983; *Franz et al*., 1993; *Vandenberg and Lister*, 1996; *Gupta and Bickle*, 2004; *Huet et al*., 2009; *Huet*, 2010]. In addition, synorogenic top-to-the-south overthrusting relationships between the Cycladic Blueschists in the hanging wall and the Cycladic Basement unit in the footwall were recently described on Ios [*Huet et al*., 2009] after a long debate on the relative timing and the kinematics of the South Cycladic shear zone [see *Lister et al*., 1984; *Vandenberg and Lister*, 1996]. The Cycladic Blueschists/Cycladic Basement contact, which is also exposed on Sikinos [*van der Maar et al*., 1981; *Franz et al*., 1993], has not been the subject of a comparable study.

Rocks of the Cycladic Blueschists and the Cycladic Basement units were both exhumed during two distinctive stages in two contrasted settings [*Ring et al*., 2011; *Jolivet and Brun*, 2010; *Grasemann et al*., 2012]. The first stage occurred in the Hellenic subduction context during the Eocene, burial and exhumation of eclogite and blueschist-facies assemblages [e.g., *Altherr et al*., 1979; *Wijbrans and McDougall*, 1986; *Bröcker and Franz*, 1998; *Trotet et al*., 2001a, 2001b; *Groppo et al*., 2009] in a subduction channel or extrusion wedge structure [*Jolivet et al*., 2003; *Jolivet and Brun*, 2010; *Ring et al*., 2007a, 2010; *Huet et al*., 2011]. Basal parts of the Cycladic Blueschists unit reached a common, similar peak-metamorphic conditions of approximately 18–20 kbar for 500–500°C, some 45–35 Ma ago throughout the Cycladic Archipelago [e.g., *Trotet et al*., 2001a; *Parra et al*., 2002; *Ring et al*., 2007b; *Huet*, 2010]. The second stage occurred in the back-arc domain, during the Oligocene and Miocene postorogenic extension. During this stage, both the Cycladic Basement and the Cycladic Blueschists units were exhumed in metamorphic domes or Cordilleran-type MCCs [*Lister et al*., 1984] below a series of detachments showing dominant top-to-the-north or -NE kinematics [e.g., *Avigad and Garfunkel*, 1989; *Buick and Holland*, 1989; *Buick*, 1991; *Faure et al*., 1991; *Lee and Lister*, 1992; *Gautier et al*., 1993; *Gautier and Brun*, 1994a; *Jolivet and Patriat*, 1999; *Vanderhaeghe*, 2004; *Kumerics et al*., 2005; *Mehl et al*., 2005, 2007; *Denèle et al*., 2011]. In the Northern Cyclades, a set of distinct detachments was recently grouped in a single

large-scale structure cropping out over up to 130 km to form the North Cycladic Detachment System (NCDS) (Figure 1) [*Jolivet et al*., 2010] resulting in a general asymmetric picture of the Aegean domain. A similar set of detachments with opposed, top-to-the-south or -SW kinematics was identified in the Western Cyclades [*Grasemann and Petrakakis*, 2007; *Iglseder et al*., 2009, 2011; *Tschegg and Grasemann*, 2009; *Brichau et al*., 2010] and recently mechanically linked to form the West Cycladic Detachment System (WCDS), resulting in a more symmetrical picture of the Aegean domain [*Grasemann et al*., 2012]. Late exhumation stages along both extensional systems were accompanied by the emplacement of syntectonic Miocene I and S-type granites (i.e., Tinos, Mykonos, Ikaria, Naxos, Serifos, or even Lavrio; see Figure 1) [*Jansen*, 1973; *Lee and Lister*, 1992; *Altherr and Siebel*, 2002; *Grasemann and Petrakakis*, 2007; *Iglseder et al*., 2009; *Bolhar et al*., 2010].

2.2. Geology of the Southern Cyclades

Sikinos and Folegandros are located in the central part of the Aegean Sea, and together with Ios form the Southern Cyclades. These islands dispose of a recent map coverage performed by the Greek geological survey [*Avdis and Photiades*, 1999], complemented for Folegandros, by independent geological mapping [*Sowa*, 1985]. However, at variance with Ios located only 7 km east of Sikinos, the tectonometamorphic evolution of Sikinos and Folegandros remains fragmentary and unevenly known.

Just as Ios, the metamorphic succession of Sikinos and Folegandros consists in the tectonic superimposition of two distinct tectonometamorphic units, the Cycladic Blueschists and Cycladic Basement units [*van der Maar*, 1980; *van der Maar and Jansen*, 1983; *Franz et al*., 1993; *Avdis and Photiades*, 1999; *Gupta and Bickle*, 2004].

Outcrops of the Cycladic Basement unit are restricted to the Southeastern coast of Sikinos in two tectonic windows surrounded by the Cycladic Blueschists unit [e.g., *van der Maar*, 1980]. The first-order architecture of the Cycladic Basement unit appears quite similar to the one described on Ios with a mylonitic carapace mantling a relatively less deformed core [e.g., *Huet et al*., 2009]. Similarly, basement lithologies include variably deformed metasediments and metagranitoid stocks [*van der Maar*, 1980; *van der Maar and Jansen*, 1983; *Franz et al*., 1993]. Metasediments consist mostly in garnet-micaschists and gneisses preserving relics of amphibolite-facies mineral assemblages equilibrated at conditions of approximately 570–650°C for 5 kbar [e.g., *van der Maar*, 1980; *Franz et al*., 1993]. Interestingly, these rocks are intruded by variably oriented aplite dykes and a granodiorite pluton recently dated at approximately 310 Ma [*Photiades and Keay*, 2003]. This Variscan heritage is variably overprinted by a two-step alpine tectonometamorphic evolution [e.g., *van der Maar and Jansen*, 1983; *Franz et al*., 1993; *Gupta and Bickle*, 2004]. While former Variscan mineral assemblages and associated structures are preserved in large parts of the Cycladic Basement, the alpine metamorphic overprint appears spatially restricted to the most strained rocks of the mylonite carapace. This correlation has been interpreted as the result of localized deformation-enhanced fluid percolations in the vicinity of the Cycladic Blueschists/Cycladic Basement contact [*Gupta and Bickle*, 2004]. The discrete crystallization of HP-LT index minerals such as glaucophane, chloritoid, or garnet and high-silica content phengite [*van der Maar*, 1980; *Henjes-Kunst and Kreuzer*, 1982; *van der Maar and Jansen*, 1983] yielded Eocene peak-metamorphic conditions evaluated to 480 ± 20°C and 11 kbar [*van der Maar and Jansen*, 1983; *Andriessen et al*., 1987; *Baldwin*, 1996; *Baldwin and Lister*, 1998; *Gupta and Bickle*, 2004]. It is noteworthy that this estimate falls well below recent, approximately 16.5 kbar for 550°C estimates performed on Ios as retrieved from a pseudosection approach [*Huet*, 2010]. Rocks further recrystallized in the greenschist-facies conditions in the upper parts of the mylonite carapace [e.g., *van der Maar*, 1980; *Gupta and Bickle*, 2004]. This retrogression event may have occurred between 30 and 25 Ma as dated on Ios [*van der Maar and Jansen*, 1983; *Andriessen et al*., 1987; *Baldwin and Lister*, 1998; *Huet*, 2010].

The Cycladic Blueschists unit is exposed on both Sikinos and Folegandros as a approximately 6–7 km thick association of metasediments including micaschists and marbles layers and minor metabasite occurrences [*van der Maar and Jansen*, 1983; *Avdis and Photiades*, 1999] whose emplacement within the series was recently dated between 225 and 200 Ma [*Photiades and Keay*, 2003]. At variance with the underlying Cycladic Basement unit, blueschists and more locally eclogitic parageneses developed throughout the metamorphic succession and are often at least partially preserved within more retrograded rocks [*Avdis and Photiades*, 1999; *Photiades and Keay*, 2003]. P-T conditions retrieved for peak-metamorphic conditions yielded 11–14 kbar for 480 ± 20°C that, again, strongly contrast with results obtained on similar assemblages in the neighboring islands [i.e., *Trotet et al*., 2001b; *Parra et al*., 2002; *Groppo et al*., 2009; *Huet*, 2010]. Another difference with surrounding islands is the subdivision of the Cycladic Blueschists unit in a set of subunits separated by tectonic

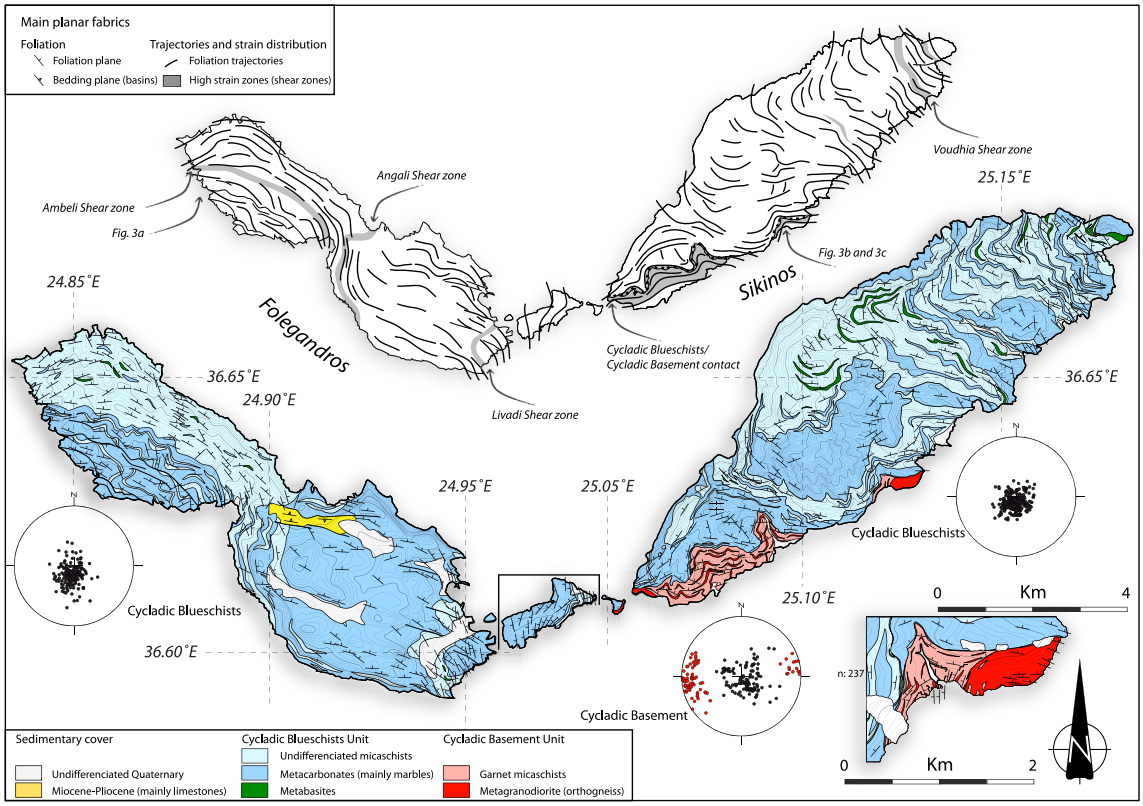

Figure 2. Main planar fabrics of Sikinos and Folegandros islands. Geological and foliation map of Sikinos and Folegandros islands. Lithologic outlines are from new field observations and a compilation of existing maps [e.g., *Sowa*, 1985; *Avdis and Photiades*, 1999]. Poles of foliation in both the Cycladic Blueschists and the Cycladic Basement units are presented in Schmidt's lower hemisphere equal-area projection. Detailed map of the northern tectonic window of the Cycladic Basement unit surrounded by the Cycladic Blueschists unit. Note that the geometry of the main foliation remains constant across the Cycladic Blueschists/Cycladic Basement contact. Simplified geological map showing foliation trajectories and traces of the main shear zones. Also indicated is the position of the pictures of Figure 3.

contacts [*Avdis and Photiades*, 1999]. It has even been proposed that the uppermost subunit of Folegandros was only equilibrated in the greenschist-facies conditions [*Avdis and Photiades*, 1999]. However, quantitative P-T estimates are currently missing. While a general top-to-the-north sense of shear is proposed in a large-scale review [e.g., *Gautier et al*., 1993], neither the kinematics nor the metamorphic conditions that prevailed during the activity of these contacts are known. Similarly, despite an obvious potential tectonic importance, the nature and evolution of the Cycladic Blueschists/Cycladic Basement contact remain poorly studied. Mostly devoted to petrological and fluid channeling concerns, the study of *Gupta and Bickle* [2004] proposed a general top-to-the-south sense of shear.

3. Finite Structure and Distribution of Metamorphic Markers

An extensive field survey was carried out on Sikinos and Folegandros islands, including field mapping in order to complement the existing G-IGME geological maps [*Avdis and Photiades*, 1999]. Results are shown in Figure 2; readers are referred to the existing maps [*Sowa*, 1985; *Van der Maar et al*., 1981; *Franz et al*., 1993; *Avdis and Photiades*, 1999] to appreciate the changes.

In addition to a thin Neogene to recent sedimentary cover, dominant lithologies were distinguished within the Cycladic Blueschists unit and the Cycladic Basement irrespectively of the metamorphic grade or the finite strain experienced by the rocks. Accordingly, three main lithologies, including marbles (calcite and dolomite marbles, carbonate-rich metaconglomerates), micaschists (including calcschists and minor metaquartzites), and metabasites, were mapped within the Cycladic Blueschists unit. In the Cycladic Basement unit, only two main lithologies were distinguished; metapelites (micaschists, gneisses, and minor metaquartzites) and variably strained orthogneiss bodies derived from Variscan granodioritic stocks. The main tectonic features having a map-scale expression were also reported (Figure 2). These structures consist primarily in the Cycladic

Blueschists unit-Cycladic Basement contact and in a limited number of ductile to ductile-brittle shear zones and brittle fault zones.

Geological mapping was complemented by a detailed study of both structural and metamorphic features of the islands. The structural analysis consists primarily in the study of both the main planar fabrics and the stretching lineations. In parallel, large-scale analysis of the distribution of the metamorphism allows constraining physical conditions that prevailed during deformation. Asymmetry of the deformation is presented for the Cycladic Blueschists unit in section 4 and for the Cycladic Basement unit in section 5. Analysis of brittle structures is presented in section 6. Quantitative estimates of peak-metamorphic conditions for the main units are presented in section 7.

3.1. Structural Analysis

Finite strain markers including foliation, stretching lineation, and fold geometry were studied over 787 stations; 505 on Sikinos (including 266 stations within the Cycladic Basement) and 282 on Folegandros. All metamorphic rocks of both units and part of the orthogneiss bodies are pervasively foliated and generally exhibit conspicuous stretching lineation allowing the accurate determination of the orientation of the planar-linear fabric. Detailed results including maps of finite strain markers, foliation trajectories, and field measurements stereoplots are presented in Figures 2 and 4.

3.1.1. Main Planar Fabrics

Compositional layering in the metasediments of both units has been generally completely transposed into a main penetrative foliation. The first-order geometry of the islands thus appears quite well in the landscape. Recumbent isoclinal folds that are responsible for this transposition were only observed in low-strain domains, particularly within thick marble layers (Figure 3a). Such an incomplete transposition is also visible at the scale of the map by locally oblique foliation trajectories (Figure 2). Conversely, the main foliation tends to increase in intensity toward the Cycladic Blueschists/Cycladic Basement contact and in the NE of Folegandros where a tectonic contact may occur offshore. These large-scale strain gradients are further complicated by more local strain localization over a limited number of ductile shear zones within the Cycladic Blueschists unit [*Avdis and Photiades*, 1999]. Shear zones developed, in most cases, at shallow angle or even parallel to the lithological layering as foliation-parallel shear zones or décollement zones in weak, generally metapelitic lithologies. Deformed zones can be followed along several kilometers (about 5 km for the Ambeli shear zone) for typical thickness of about 20–30 m and locally reach approximately 50 m (Figure 2). Less important shear zones proposed on the geological map [*Avdis and Photiades*, 1999] were abandoned. We thus distinguished, from bottom to top, the Voudhia shear zone in the northeastern part of Sikinos that roofs most of the structural succession and the Ambeli, Angali, and Livadi ductile shear zones that divide the structure of Folegandros (Figure 2).

Orientation of 752 foliation planes were measured, 487 on Sikinos and 265 on Folegandros in all lithologies of the two main tectonic units (Figure 2). Foliation trajectories over the two islands and a more detailed map embracing the northern Cycladic Basement occurrence are given in Figure 2. At a first glance, the main foliation depicts a north to NE dipping monocline on both islands (Figure 2). The different orientations of the islands with respect to the average dip direction thus explains striking differences of the metamorphic series: elongated NE-SW, Sikinos displays a thick metamorphic succession of the Cycladic Blueschists unit and the upper part of the Cycladic Basement, while the NW-SE orientation of Folegandros only allows a thin segment of the Cycladic Blueschists unit to crop out. In further details, the main foliation is affected by a series of large-scale open upright folds with gently north plunging axes allowing the Cycladic Basement unit to crop out at the favor of two structural antiforms. There, the foliation draws an overall concentric pattern around the Cycladic Basement as observed in Ios [*van der Maar*, 1980; *van der Maar and Jansen*, 1983; *Vandenberg and Lister*, 1996; *Forster and Lister*, 1999a; *Huet et al*., 2009]. Such a large-scale folding, known in most islands of the Aegean domain, may correspond to a constriction component during the final exhumation stage of the Cycladic Blueschists unit or to a late shortening event [e.g., *Jolivet et al*., 2004; *Menant et al*., 2013]. Foliation dip varies from 0 to 90°. Foliation in the Cycladic Blueschists unit generally displays gentle dips with a very low dispersion (Figure 2). Mean dip value is about $19 \pm 7°$ on Sikinos while it reaches about $29 \pm 11°$ on Folegandros (Figure 2). Conversely, the Cycladic Basement presents two drastically different fabrics (Figures 2 and 3b). Thanks to good outcrop conditions, relationships between these two fabrics were studied in detail along the cliffs located of the northern occurrence of the Cycladic Basement

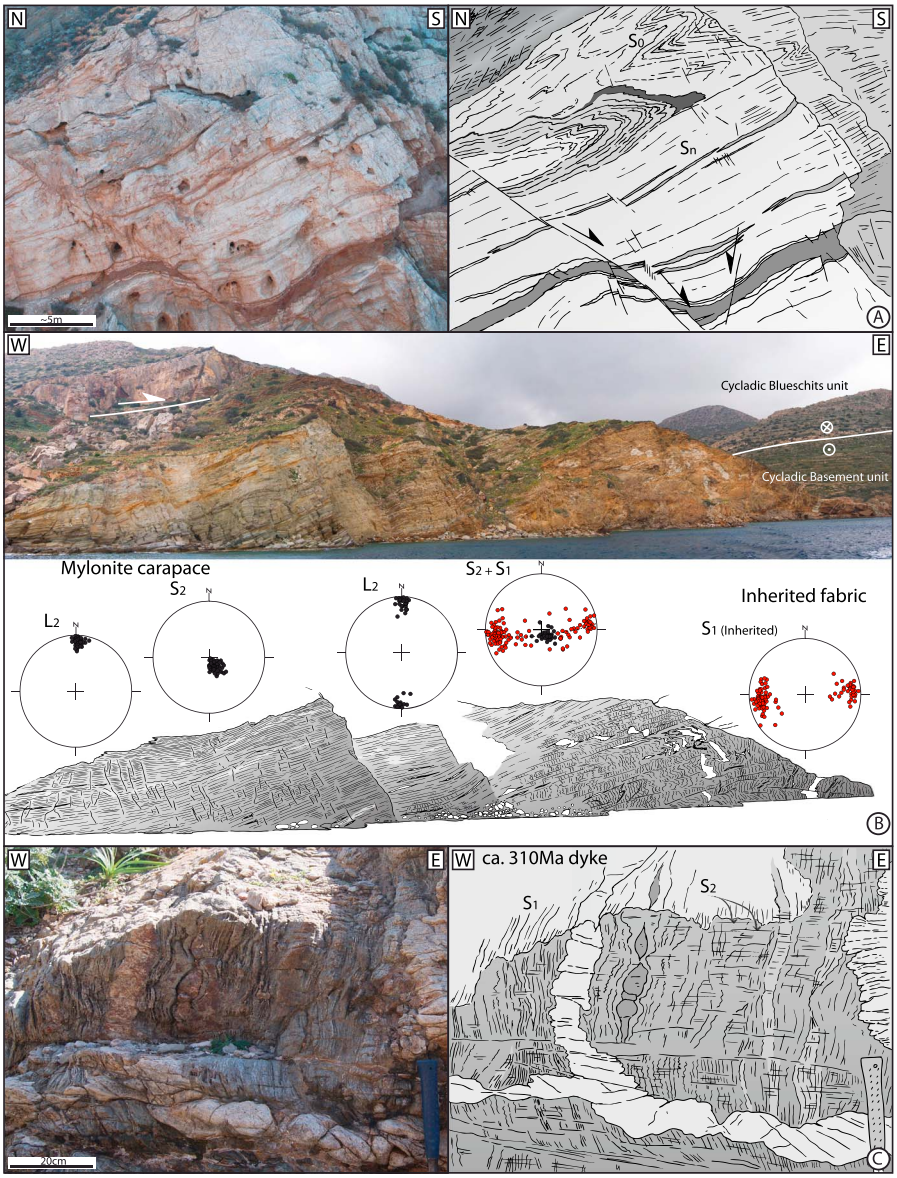

Figure 3. Relationships between the main planar fabrics. (a) Incomplete transposition of the compositional layering (i.e., initial bedding) into a main, flat-lying penetrative foliation in a marble layer, southwest of Folegandros. Note the presence of ductile-brittle and brittle extensional structures consistent with a north-south stretching. (b) Transposition of the Variscan steeply dipping foliation that characterizes the core of the Cycladic Basement unit into the flat-lying penetrative foliation of the mylonite carapace in the vicinity of the Cycladic Blueschists/Cycladic Basement contact. Note the attitude of the circa 310 Ma granodiorite dykes that are quite illustrative of the amount of strain experienced along the contact. (c) Close-up view of the crosscutting relationships between the Variscan foliation and the late Variscan granodiorite dykes. The intrusive character of the granodiorite bodies within the wall rocks ensures an inherited character for this steeply dipping fabric. Note the incipient vertical thinning coeval with the transposition of the vertical fabric that overprints an initial (Variscan) vertical stretching. See Figure 2 for location.

unit, and three different domains were distinguished from bottom to top on the basis of their structural features and their relationship with intrusive rocks (Figure 3b). The first domain, in the deepest parts of the Cycladic Basement, is characterized by a N170 striking, steeply dipping to vertical, high-grade foliation in the garnet-micaschists traversed by vertical granodioritic dykes of various scales (Figures 3b and 3c). The intrusive character of the circa 310 Ma old granitoid bodies thus unambiguously ensures a Variscan age for this fabric [*Photiades and Keay*, 2003]. The magmatic rock remains devoid of a significant strain, while the garnet-micaschists are characterized by an incipient flat to gently dipping Alpine foliation (Figure 3c). The

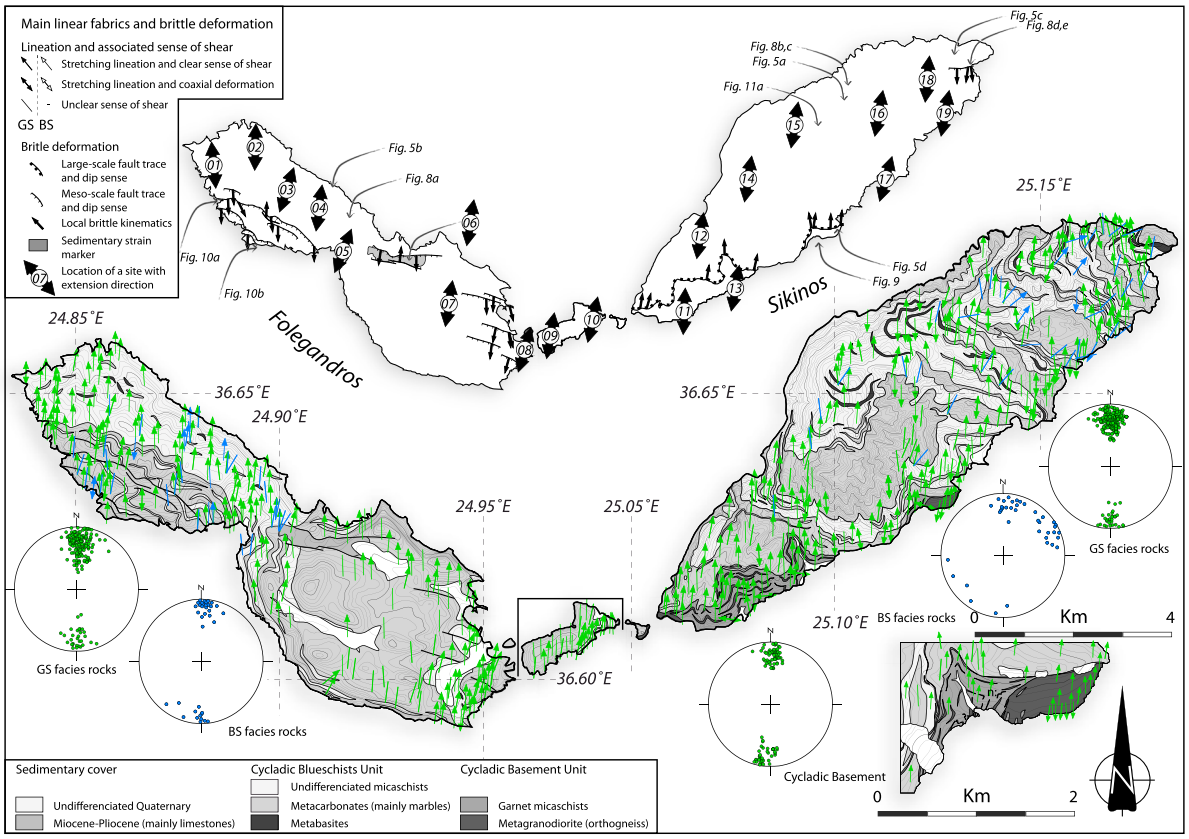

Figure 4. Stretching lineations of Sikinos and Folegandros islands. Geological and stretching lineation map of Sikinos and Folegandros Islands. Stretching lineations in both the Cycladic Blueschists and the Cycladic Basement units are presented in Schmidt's lower hemisphere equal-area projection. Lineations associated to blueschist-facies rocks are indicated in blue; lineations associated to greenschist-facies rocks in green either on the map or on the projections. Detailed map of the northern tectonic window of the Cycladic Basement unit surrounded by the Cycladic Blueschists unit. Note that the orientation of the stretching lineation remains constant across the Cycladic Blueschists/Cycladic Basement contact. In addition, both top-to-the-north and top-to-the-south senses of shear are present in the Cycladic Basement unit (see text for details). Simplified geological map showing the results of the fault slip data inversion together with traces of main brittle structures and their local kinematics. Also indicated is the position of the pictures of Figures 5 and 8–11.

second domain, located at the top of the cliffs, presents two distinctive foliations. The former Variscan foliation is variably preserved in lense-shaped domains and is involved in recumbent isoclinal folds associated with the development of a crenulation cleavage with a low (~20°) dip. This domain is thus characterized by an intense vertical shortening, and a north-south lineation is only well developed where the crenulation cleavage is best expressed (Figure 3b). The last domain, the mylonite carapace corresponds to the last approximately 100 m uppermost parts of the Cycladic Basement and is only characterized by a single strong foliation marked by greenschist-facies assemblages. There, the Variscan foliation and the dykes are completely transposed into the mylonitic fabric whose intensity drastically increases toward the Cycladic Blueschists/Cycladic Basement contact. It is thus noteworthy that the geometry of the main foliation (i.e., strike and dip) remains constant across the Cycladic Blueschists/Cycladic Basement contact (Figures 2 and 3b).

3.1.2. Stretching Lineations

Stretching lineation is a common feature of the metamorphic rocks of Sikinos and Folegandros Islands (Figures 4 and 5). It is defined by various markers, depending on the nature of the protolith, metamorphic grade, and strain intensity (Figure 5). Lineation is, however, more ambiguous within the thick (dolomite) marble layers where compositional layering often interferes with the main metamorphic foliation or into the less deformed (i.e., the deeper) parts of the Cycladic Basement unit, particularly within the orthogneiss bodies that locally present no significant strain.

Orientation of 649 stretching lineations has been measured throughout the islands (404 on Sikinos and 245 on Folegandros) in all lithologies of the two main tectonic units (Figure 5). On most outcrops, the orientation

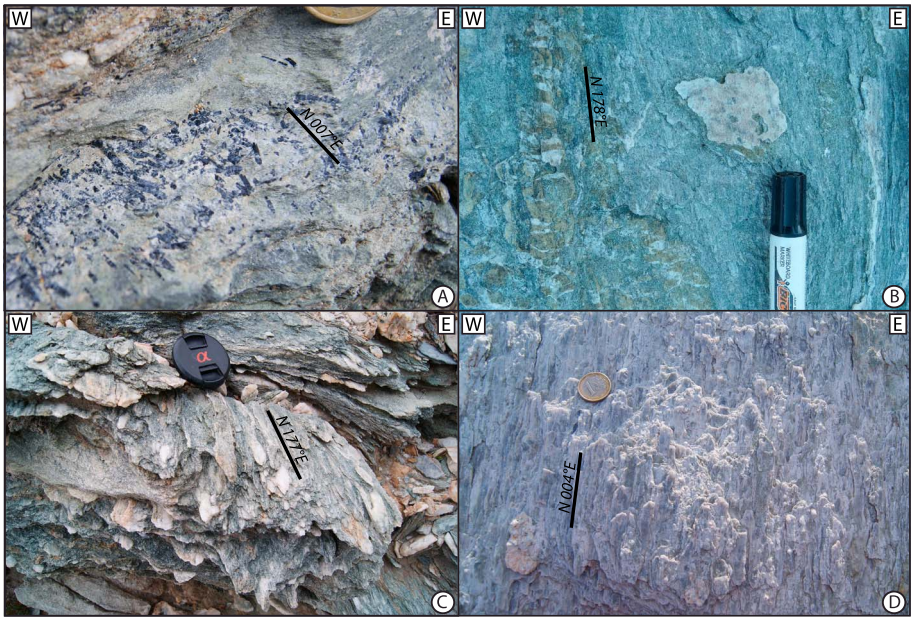

Figure 5. Stretching indicators. (a) Elongation and truncation of large blue-amphibole crystals in a fresh blueschist. (b) Stretching of epidote-rich layers in a partially retrogressed blueschist in the greenschist-facies conditions. Stretching lineation is also marked by the elongation of chlotite aggregates that have grown between stretched blue-amphiboles. (c) Typical conglomerate marble on the northeastern part of Sikinos. Stretching is marked by the elongation of the calcite pebbles embedded in a more politic matrix. (d) In the orthogneiss of the Cycladic Basement unit, stretching lineation is outlined by the elongation of inherited magmatic minerals (mostly K-feldspar and quartz) and by the growth of phyllosilicates and locally tourmaline over the foliation plane. See Figure 4 for location.

of the stretching lineation appears fairly constant with a rather low dispersion. Associated with the crystallization of large amounts of synkinematic chlorite and albite, stretching was clearly recorded within greenschist-facies metamorphic conditions. The case of rocks devoid of significant synkinematic retrogression, consequently best preserving blueschist-facies conditions, was treated separately. In the Cycladic Blueschists unit, stretching lineation is outlined by stretched quartz rods, the direction of strain shadows, and more routinely by elongated phyllosilicate aggregates such as white micas and chlorite. More rarely, stretching is marked by the elongation of stretched pebbles in the metaconglomerate layers (to the north of Sikinos). On Folegandros, the orientation of the stretching lineation is centered on an average value of N004 with a dominant (i.e., 87%) northward plunge (Figure 4). On Sikinos, the orientation of the stretching lineation in the Cycladic Blueschists unit is centered on an average value of N001 and shows very low dispersion (Figure 4). Eighty-four percent of the lineations have a northward plunge with an approximately 15° mean dip angle (Figure 4).

Stretching lineation in blueschist-facies rocks is generally marked by the alignment and the truncation of prismatic minerals such as glaucophane and epidote. Direction of stretching appears rather scattered, and the accurate determination of a preferred stretching direction prevailing during blueschist-facies conditions is hindered by the poverty of the data set (only 41 measurements on Sikinos and 38 measurements on Folegandros). On Sikinos, where HP rocks are best expressed compared to Folegandros, the trend is more dispersed with a well-defined approximately north-south cluster of lineations and a more NE-SW centered one.

In the Cycladic Basement, stretching lineation is outlined by the elongation of inherited magmatic minerals (mostly K-feldspar and quartz) and by the growth of phyllosilicates and tourmaline in the foliation plane in the orthogneiss (Figure 5d). In the surrounding garnet-micaschists, the stretching lineation is mostly outlined by phyllosilicates and chlorite pressure shadows around garnet or synkinematic albite. Orientation of the stretching lineation in the basement is centered on an average value of N006 and shows very low dispersion (Figure 4). Preferred stretching direction becomes less clear and then completely disappears in the core of the basement unit. It is therefore noteworthy that both units recorded a common approximately north-south stretching at least during retrogression of HP parageneses in the greenschist-facies conditions.

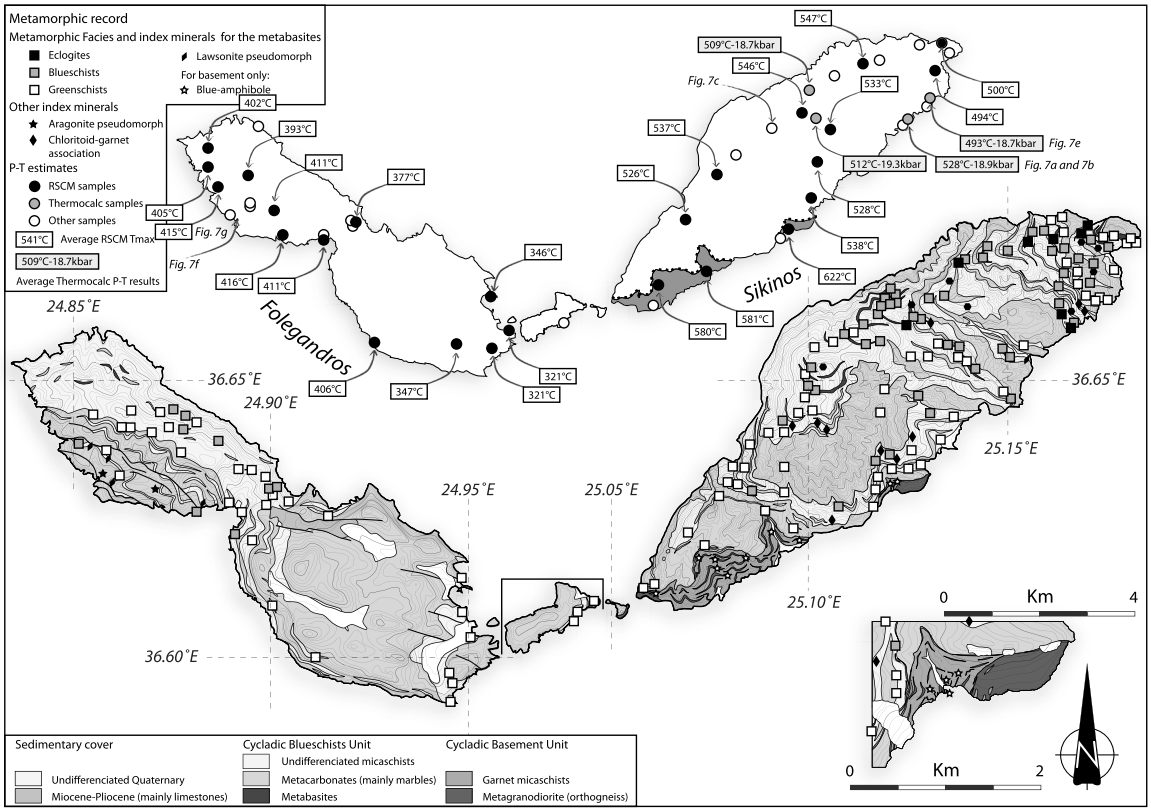

Figure 6. Metamorphic record on Sikinos and Folegandros Islands. Geological, metamorphic facies, and mineral occurrences map of Sikinos and Folegandros Islands. The metamorphic facies in metabasites of the Cycladic Blueschists unit is indicated by the color of the square: eclogite (black), fresh blueschist (grey), and greenschist (white) together with occurrences of other index minerals. Detailed map of the northern tectonic window of the Cycladic Basement unit surrounded by the Cycladic Blueschists unit. Note the presence of a quite well-preserved prealpine amphibolite-facies assemblage in the Cycladic Basement unit [e.g., *van der Maar*, 1980; *Franz et al*., 1993]. Simplified geological map showing the results of the P-T constraints. Samples used for RSCM Tmax purposes appear as black circles, average P-T as grey circles, and other samples as white circles. Also indicated is the position of the pictures of Figure 7.

3.2. Distribution of the Metamorphic Record

The metamorphic record was investigated throughout the two islands. Parageneses in metabasites, which are a straightforward field indicator of P-T conditions in the sense of *Eskola* [1920], were particularly studied. This analysis was strengthened by the recognition of index minerals in other types of rocks including chloritoid, lawsonite, or aragonite in metapelites or calcschists whether preserved or pseudomorphosed. All results are presented in Figure 6, and some representative field examples are given in Figure 7.

"Pure" metabasites are often turned to eclogite bodies dominated by omphacite only scarcely associated with garnet (Figures 7a and 7b) and present two distinctive steps of retrogression. The first step is characterized by the progressive replacement of omphacite by randomly oriented blue-amphiboles along the rims of eclogites boudins (Figure 7a). Crystallization also occurred along calcite (after aragonite) veins where blue-amphiboles present an approximately north-south preferred orientation (Figure 7b). In those lithologies, blueschist-facies is thus secondary as already pointed out in Ios [*Forster and Lister*, 1999b; *Huet et al*., 2009]. The second retrogression step, locally responsible for the complete destabilization of former HP assemblages occurred in the greenschist-facies conditions while rocks experienced strongly noncoaxial deformation. Rocks are characterized by a strong chlorite-albite foliation, a north-south lineation and a conspicuous top-to-the-north asymmetry (Figure 7c). Rocks of intermediate composition generally appear as glaucophane-garnet micaschists (Figure 7d). Metapelites routinely develop chloritoid-garnet assemblages (Figure 7e) showing, at least, an incipient greenschist-facies retrogression. Most of the metacarbonates do not provide any information observable on the field except for the presence of pseudomorphs after aragonite, while impure marbles often developed blue-amphibole-phengite assemblages (Figure 7f). Fresh lawsonite is never preserved and always occurs as lozenge-shaped pseudomorphs (Figure 7g). HP

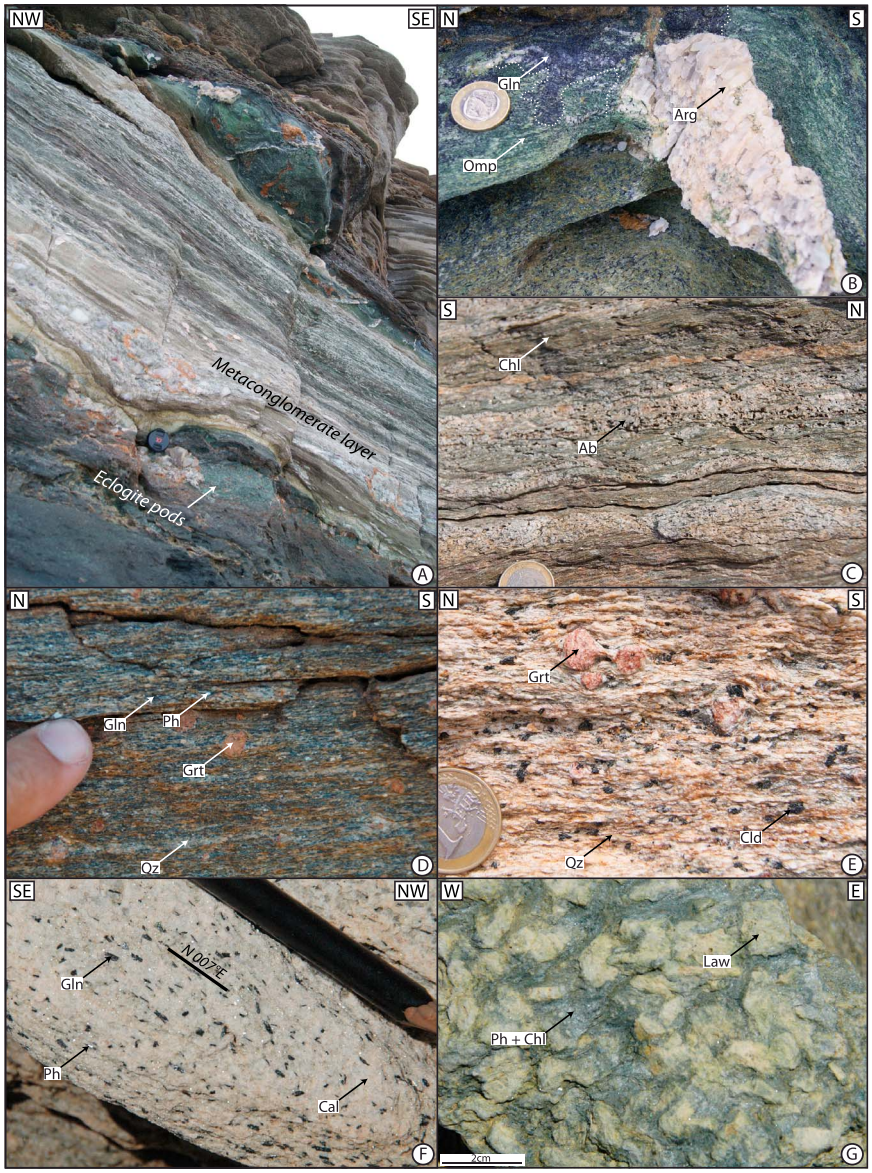

Figure 7. Metamorphic record on Sikinos and Folegandros Islands. (a) Typical outcrop conditions of the eclogite pods to the north of Sikinos. Metabasites often occur as dismembered "rounded" pods from several tens of centimeters in length intercalated within the metamorphic series. Massive omphacite pods are often invaded from the rims by randomly oriented blue-amphiboles. (b) Close-up view of a part of an omphacite pod in the vicinity of a calcite vein (pseudomorph after aragonite) along which retrogression in the blueschist-facies is intense. There, blue-amphibole often presents an approximately north-south preferred orientation. (c) Heavily retrogressed metabasites in the greenschist-facies conditions. The rock is turned into a well-foliated chl-alb prasinite showing clear top-to-the-north shear criteria. (d) Detailed view of an outcrop of micaceous "glaucophanites" where sample Sik09006 has been selected. The mineralogy comprises in order of decreasing abundance gln + ph + grt + qz + pg + rt + chl ± ctd. (e) Detailed view of a typical outcrop of grt-ctd metapelites where sample Sik11266 was selected. These rocks show incipient synkinematic recrystallizations in the greenschist-facies conditions. (f) Ph-gln marble showing a preferred approximately north-south orientation of the blue-amphiboles (gln). (g) Outcrop of metabasites showing Ep-chl-ph pseudomorphs after lawsonite. Mineral abbreviations are after *Whitney and Evans* [2010]. See Figure 6 for location.

assemblages in the Cycladic Basement unit are very limited due to ubiquitous greenschist-facies retrogression. Conversely, a prealpine amphibolite-facies assemblage is locally quite well preserved as already shown by *van der Maar* [1980] and *Franz et al.* [1993]. Blue-amphibole-garnet assemblages are, however, present at the base of the mylonite carapace (Figure 6). Chloritoid-blue-amphibole assemblages, described in *Gupta and Bickle* [2004] have not been recognized.

Rocks of the Cycladic Basement unit and of the Cycladic Blueschists unit on the two islands experienced a HP-LT event. Blue-amphibole and pseudomorphs after lawsonite argue for typical subduction-related high P/T ratio [e.g., *Agard and Vitale-Brovarone*, 2013]. Depending on (i) the ability of the protolith to develop HP index minerals, (ii) peak-metamorphic conditions, or (iii) the intensity of retrogression, distribution of HP rocks is, however, highly heterogeneous (Figure 6). On Sikinos, preservation of the HP metamorphism is locally quite exemplary and is reminiscent of outcrops of Syros or Sifnos [e.g., *Trotet et al*., 2001a, 2001b; *Parra et al*., 2002; *Schumacher et al*., 2008; *Groppo et al*., 2009]. Eclogites (Figures 7a and 7b) and more routinely blue-amphibole micaschists (e.g., Figure 7d) or chloritoid-garnet micaschists (Figure 7e) are thus quite common and generally well preserved (Figure 6). A strong correlation between the occurrence of greenschist-facies rocks and concentration of strain (compare Figure 7b and Figure 7c) was often observed from the scale of the outcrop to the scale of the thin section (Figures 8a–8c). The same correlation is even detectable at large scale as retrogression is more complete along the main shear zones (i.e., the Voudhia shear zone, Figure 8d) and the Cycladic Blueschists/Cycladic Basement contact (Figure 6). There, HP mineral associations are heavily destabilized and replaced by typical greenschist-facies assemblages (Figure 8e).

HP mineral assemblages were also observed on Folegandros. Blueschist-facies rocks are locally abundant, and pseudomorphs after both lawsonite and aragonite are quite common (i.e., Figures 7b and 7g). However, the most striking difference compared with the metamorphic record of Sikinos is the total absence of garnet in any type of rocks throughout the island. The lack of garnet at that scale argues that temperature may have not exceeded approximately 450°C [e.g., *Spear*, 1993; *Bosse et al*., 2002], and it is thus tempting to ascribe lower peak-metamorphic temperature conditions to Folegandros than to Sikinos. In more details, internal distribution of HP mineral assemblages appears restricted to the NW part of Folegandros as if the Angali shear zone corresponds to the blue-amphibole and the lawsonite metamorphic isograds (Figure 6). Rocks from the SE part of Folegandros thus appear as low-grade metasediments where chlorite appears as the unique conspicuous metamorphic mineral and, conversely, Late Jurassic to Early Cretaceous foraminiferal assemblages are still preserved [*Avdis and Photiades*, 1999].

4. Kinematics of Deformation in the Cycladic Blueschists Unit

4.1. A Pervasive Top-to-the-North Sense of Shear as the Main Record

The whole Cycladic Blueschists unit is affected by a pervasive top-to-the-north ductile deformation. Kinematic indicators of top-to-the-north deformation are very common and often unambiguous at all scales (Figure 8). Shear bands are among the more ubiquitous simple shear criteria. Normal-sense, top-to-the-north shear bands are particularly abundant in the metapelites, calcschists, and part of the metaconglomerate layers. Their spacing ranges from few millimeters in the weakest lithologies in the vicinity of main contacts to decimetres in more competent levels. Similarly, the angle between shear bands and the main foliation varies in a wide range from approximately 20–25° to more than 60°. On some outcrops, only a single set of planar, reasonably parallel shear bands developed. More rarely, several sets of shear bands may be distinguished; the steepest being often the last to form; this increasingly brittle behavior has often been explained by relative hardening of the material during progressive cooling [e.g., *Mehl et al*., 2007]. In more alternating lithologies, asymmetric deformation is accommodated by the boudinage of competent levels into a weaker, generally metapelitic matrix. Lenses of metabasites, dolomitic marbles, and metaquartzites thus occur as sigma- or delta-type porphyroclast systems [*Passchier and Simpson*, 1986] consistent with an overall top-to-the-north sense of shear. Marble layers often display only pure-shear deformation. The only notable exception concerns marble layers including dolomitic intercalations where antithetic bookshelf structures compatible with a top-to-the-north sense of shear frequently develop [*Goscombe et al*., 2004; *Grasemann et al*., 2005]. Intra-Cycladic Blueschists unit ductile shear zones are all characterized by intense top-to-the-north shear concentration (Figure 2). There, spacing between shear bands drastically decreases. Sheath folds with north-south, gently north plunging axes were recognized in strongly sheared alternating metapelites and metabasites in the vicinity of the Cycladic Blueschists unit-Cycladic Basement contact or the Voudhia shear zone.

4.2. Metamorphic Conditions of the Top-to-the-North Deformation

Metamorphic conditions that prevailed during deformation were mostly constrained in the field and strengthened by the observation of thin sections (Figure 6). At all scales, a peculiar attention was focused on

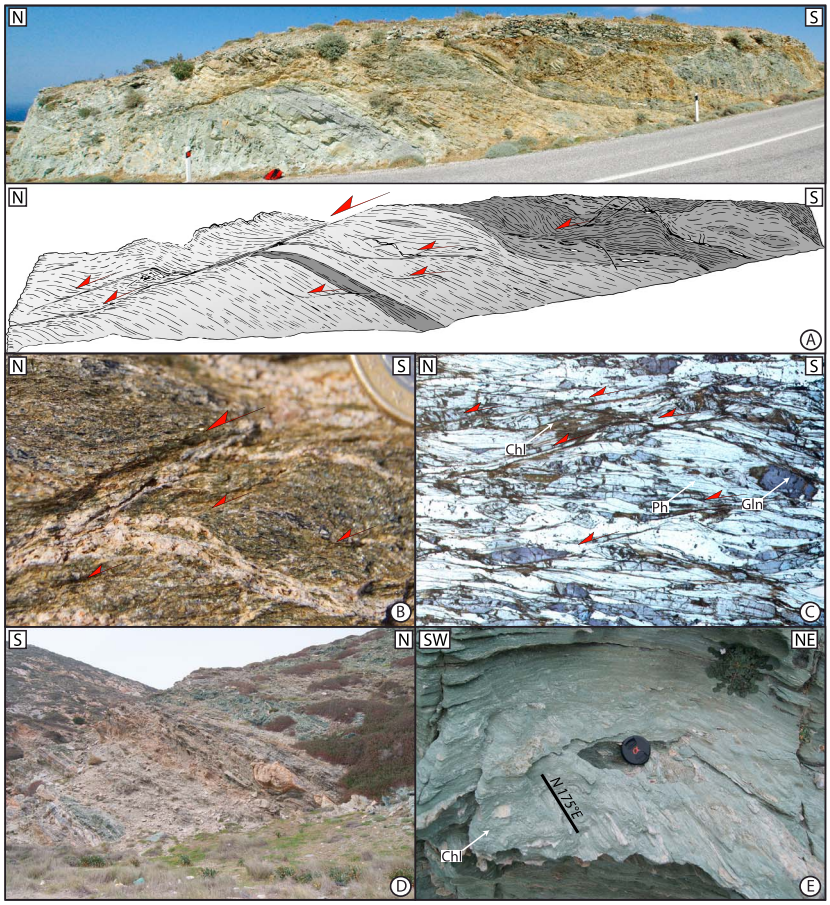

Figure 8. Metamorphic conditions of the top-to-the-north deformation. (a) Decameter-scale top-to-the-north shear band operating in the greenschist-facies conditions. HP assemblages are preserved in lense-shaped metabasites. (b and c) Small-scale top-to-the-north shear bands operating in the greenschist-facies conditions as illustrated by the synkinematic crystallization of chlorite within or in the direct vicinity of the shear bands. HP minerals (mainly blue-amphiboles and HP phengite) are passively deformed and preserved in sigmoidal foliation domains. (d) Correlation between the greenschist-facies retrogression and the presence of the top-to-the-north intra-Cycladic Blueschists Voudhia shear zone observed at the scale of the landscape. Note the presence of a 3 m long asymmetric marble boudin showing an overall top-to-the-north sense of shear. (e) Close-up view of the mylonites from the core of the Voudhia shear zone. Metabasites are turned into a chl-alb prasinite showing clear top-to-the-north shear criteria and locally sheath folds. Mineral abbreviations are after *Whitney and Evans* [2010]. See Figure 4 for location.

synkinematic minerals and more generally blastesis-deformation relationships [e.g., *Bell and Rubenach*, 1983; *Spear et al*., 1990; *Parra et al*., 2002; *Augier et al*., 2005b] which are reliable indicators of the physical conditions of deformation (Figure 8).

At the scale of the outcrop, greenschist-facies minerals appear conspicuously associated with top-to-the-north deformation (Figure 8a). In metapelites and part of the metabasites, large amounts of chlorite concentrate along shear bands or in the neck between boudins while rosette-shaped chlorite also forms in tension gashes in more resistant lithologies (e.g., Figures 5a and 5b or Figures 8b and 8c). Conversely, HP associations are preserved in sigmoidal foliation domains preserved from severe shearing at various scales (Figure 8). Fresh blueschists or even eclogites thus occur as boudins surrounded by retrograde rims (Figure 7).

Similar correlation between the greenschist-facies retrogression and the presence of top-to-the-north deformation structures has been observed at map scale. Indeed, despite pervasive yet incomplete retrogression affecting entire areas, it is noteworthy that greenschist-facies rocks appear fairly aligned along the main contacts identified independently on the basis of strain concentration criterion. The Voudhia shear zone appears quite exemplary of that correlation (Figure 8). Consequently, local pervasive retrogression can be attributed to deformation along main shear zones locally accompanied by fluid circulations.

4.3. Distribution and Metamorphic Conditions of the Top-to-the-South Deformation

On Ios, penetrative top-to-the-south shearing has long been described in both the Cycladic Blueschists and the Cycladic Basement units in the vicinity of their contact [*Lister et al*., 1984; *Vandenberg and Lister*, 1996; *Forster and Lister*, 1999a]. In the Cycladic Blueschists unit, the close association between top-to-the-south kinematics and the retrogression of eclogite in blueschist-facies conditions [*Forster and Lister*, 1999b], classically interpreted as the evidence of exhumation in the subduction zone, was ascribed to the overthrusting of the Cycladic Blueschists unit over the Cycladic Basement unit [*Huet et al*., 2009]. Owing to potential tectonic consequences a particular attention was thus paid to detect top-to-the-south kinematics in the study area.

Top-to-the-south deformation was only seldom detected throughout the metamorphic succession of Sikinos and Folegandros (Figure 4). At variance with Ios, top-to-the-south appears subordinate to top-to-the-north directed sense of shear (Figure 4). More importantly, top-to-the-south is, in most cases, clearly associated with greenschist-facies conditions as illustrated by the synkinematic crystallization of large amount of greenschist-facies minerals such as chlorite and albite on shear planes, interboudin necks, and tension gashes infillings. It is therefore suggested that top-to-the-south deformation is contemporaneous with the top-to-the-north deformation. The coexistence of opposite kinematic indicators is thus ascribed to a higher degree of coaxial deformation in less deformed domains [e.g., *Mehl et al*., 2007]. Top-to-the-south kinematics is indeed absent in highly deformed domains in the vicinity of intra-Cycladic Blueschists shear zones. More locally, top-to-the-south deformation seems related with the geometry of rigid objects such as boudins even in a strongly asymmetric context. There, sometimes intense top-to-the-south deformation localizes at the rear of boudins with respect to the top-to-the-north dominant asymmetry.

5. Kinematics of Deformation in the Cycladic Basement Unit: Nature of the Cycladic Blueschists Unit-Cycladic Basement Contact

Rocks located in the close vicinity of the Cycladic Blueschists unit-Cycladic Basement contact experienced an intense deformation. The deformed zone developed at the expense of the Cycladic Basement unit is a strongly deformed, 150–200 m thick mylonitized "carapace" overlying footwall rocks where Variscan fabrics are still preserved. Most deformation within the carapace consistently indicates a strong and probably protracted top-to-the-north shearing under both ductile and later brittle conditions (Figures 3 and 9), while less deformed domains reveal top-to-the-south sense of shear.

5.1. Top-to-the-North Strain Gradient at the Top of the Cycladic Basement

In most sections, the contact between the Cycladic Blueschists unit and the Cycladic Basement is marked by a thick layer of fault rocks. Breccias, locally more than 10 m thick are mainly developed at the expense of the Cycladic Blueschists unit (Figures 4 and 9). The Cycladic Blueschists/Cycladic Basement contact is spectacularly exposed on the SE coast of Sikinos along a single lineation-parallel continuous section (see location in Figure 4). Detailed field analysis of this key section is illustrated in Figure 9. Description of the main structural features is detailed thereafter from top to bottom (i.e., north to south).

The contact between the Cycladic Blueschists unit and the Cycladic Basement is marked by breccias and fault rocks. The thickness of the breccias is approximately 3 to 5 m and reaches locally more than 10 m farther south. Clasts, reaching locally more than 2 m and mostly derived from the Cycladic Blueschists unit, are supported by a fine-grained carbonated red cement and large amount of barite attesting for important synkinematic fluid circulations (Figure 9). Brittle deformation also concentrates over another approximately 5 m thick breccias developed above a mylonitic marble layer at the base of the Cycladic Blueschists unit (Figure 4). Kinematics of the brittle deformation, which is generally clear, indicates an overall top-to-the-north motion (Figure 9).

Below, the Cycladic Basement consists exclusively of a strongly deformed orthogneiss body resulting from the deformation of the same Variscan porphyroid granodioritic protolith that is preserved in the least deformed areas [*Gupta and Bickle*, 2004]; such context is thus quite similar to Ios [*Huet et al*., 2009]. Thanks to the relative homogeneity of the protolith and the exceptional outcrop conditions, a clear ductile deformation gradient can be easily observed over an approximately 500 m long natural section along the coast (Figure 9).

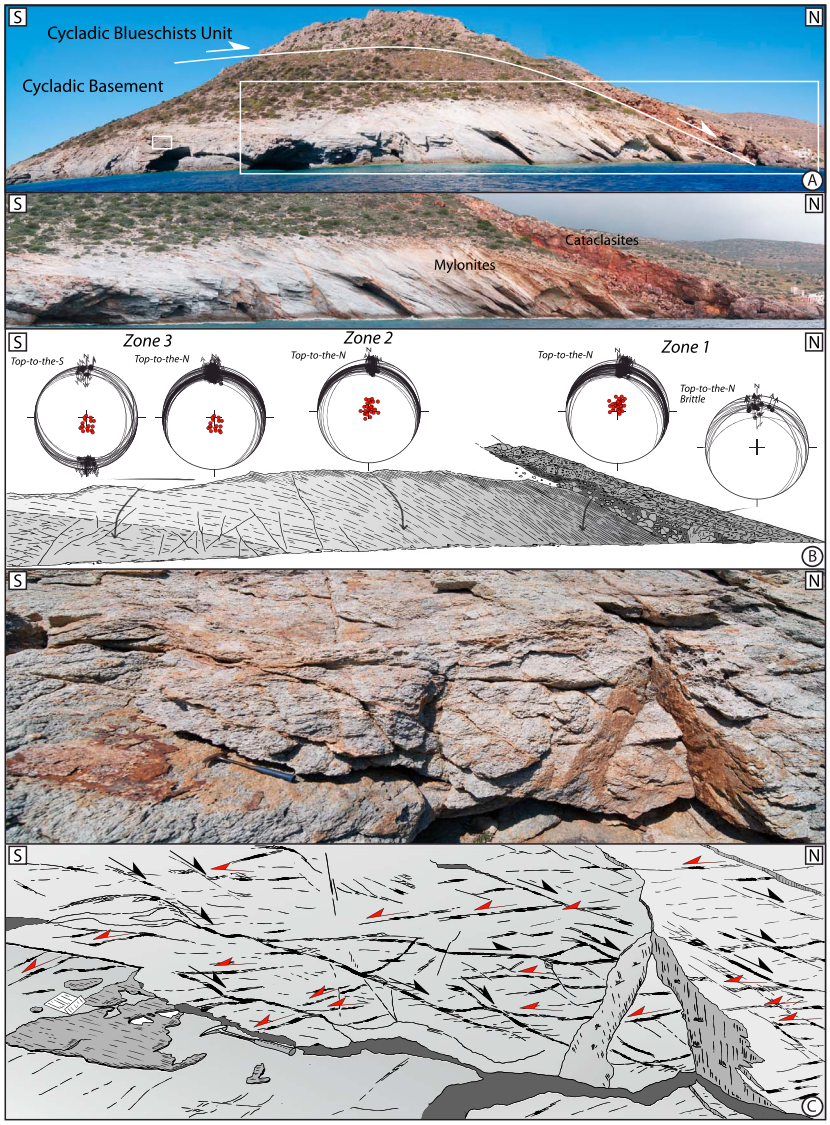

Figure 9. Kinematics of deformation in the Cycladic Basement unit. (a) Large-scale view of the Cycladic Basement/Cycladic Blueschists contact on the northern parts of the northern tectonic window of the Cycladic Basement (see location in Figure 4). The deformed zone reaches 150–200 m of thickness overlying a rather preserved footwall where even Variscan fabrics are still preserved. The mylonitized carapace shows a top-to-the-north strain ductile gradient from the south to the north. The Cycladic Blueschists/ Cycladic Basement contact is marked by a thick layer of fault rocks mainly developed at the expense of the Cycladic Blueschists unit. (b) Close-up view of contact allowing the recognition of three main deformation zones and the brittle reactivation of the contact in the brittle field (see details in the text). Poles of foliation, shear planes, and brittle fault planes are presented in Schmidt's lower hemisphere equal-area projection. (c) Zone 3, which present the less deformed rocks of the mylonite carapace is characterized by the presence of both top-to-the-north and top-to-the-south deformations. Top-to-the-north shear bands clearly crosscut former top-to-the-south ones. Note the traces of late brittle, steeply dipping normal faults that overprint ductile features. See Figure 4 for location.

Along the strain gradient, despite a rather continuous evolution of the deformation intensity, three main zones may be distinguished on the basis of criteria including the average grain size, the amount and the spacing between the shear bands, and angle between foliation and shear bands [*Agard et al.*, 2011] but also from a straightforward mineralogical evolution.

Zone 1, embracing the first approximately 30–50 m of the section, corresponds to the most ductilely deformed parts of the orthogneiss (Figure 9). There, K-feldspar and quartz are laminated, and only few K-feldspar porphyroclasts are preserved. Biotite is absent, and a large amount of newly formed chlorite and

white micas aggregates crystallize along the foliation. Proportion of white micas also clearly benefited from the strain-induced destabilization of the K-feldspar [e.g., *Gueydan et al.*, 2003]. Ultramylonites occur as thin stripes over the first approximately 10 m. Below, S-C type shear bands are very abundant and form the main structural fabric by completely obliterating the main foliation (Figure 9). Spacing between shear bands is locally as low as approximately 0.5 to 1 cm with a mean S-C angle of the order of approximately 12° (12.2 ± 6°). Kinematics of the shear bands is consistently top-to-the-north (Figure 9).

Zone 2 that spans over approximately 250 m along the coast is characterized by the progressive increasing spacing between shear bands that allows the recognition of the foliation as the main macroscopic fabric while the igneous character of the protolith is still hardly recognizable. There, the foliation is marked by the flattening of quartz and to a lesser extent of the K-feldspar. A conspicuous lineation is mostly defined by the stretching of the K-feldspar and the elongation of synkinematic aggregates of white micas and chlorite. Biotite is extremely rare, only preserved within local lower strain domains. Shear bands are generally steeper than in zone 1 with a mean angle of approximately 26° (26.2 ± 11°), reaching locally 40° with respect to the flat to gently north dipping foliation. Their spacing, of the order of 2–3 cm in the north reaches 10 to 15 cm in the south. Top-to-the-south deformation is sometimes detected at approximately 250–300 m from the contact (Figure 9).

Zone 3 is distinguished by the least deformed parts of the orthogneiss whose northern boundary corresponds to the first occurrences of weakly deformed porphyroid facies and the preservation of clear top-to-the-south kinematics. Shear bands are still abundant in the upper part of the zone and tend to space downward and finally completely disappear at approximately 500–600 m from the contact. The intrusive contact between the granite and the garnet-micaschists is thus observable at approximately 850 m from the contact.

Foliation is thus heterogeneously developed, leaving lense-shaped volumes devoid of significant subsolidus deformation whose representative dimensions increase downward. Into the lenses, the magmatic parageneses including K-feldspar, plagioclase, quartz, and metastable biotite and the preferred orientation of K-feldspar is rather diagnostic of magmatic flow than postsolidus deformation. Conversely, the lenses are wrapped into a foliation carrying a north-south stretching lineation. There, shear bands present opposite kinematics with both top-to-the-north and top-to-the-south sense of shear.

5.2. Relation and Significance of the Top-to-the-South Kinematics in the Cycladic Basement

Despite the clear dominance of the top-to-the-N deformation within the contact zone between Cycladic Blueschists unit and the Cycladic Basement, indicators of top-to-the-south deformation were observed in less strained domains. Distribution and preservation of top-to-the-south deformation thus appears closely linked with the intensity of the top-to-the-north deformation (Figure 9). This strong correlation suggests that the top-to-the-south deformation predates the development of top-to-the-north structures at large-scale and then reinforces the idea that the contact has a polyphased history such as in Ios [e.g., *Huet et al.*, 2009].

Outcrops of the upper part of zone 3 generally show the presence of both ductile and brittle structures with either top-to-the-north or top-to-the-south kinematics. However, relative chronology between top-to-the-north and top-to-the-south deformation is unambiguous. For the sake of clarity, outcrop-scale observations that are described below are located along the same section approximately 50 m from the transition between zone 2 and zone 3. A representative example is given in Figure 9c.

There, a flat or shallow-dipping foliation appears as the main fabric accompanied by a dense array of shear bands. Top-to-the-south deformation is characterized by thin either flat or shallow north dipping reverse shear bands or gently south dipping extensional shear bands. Conversely, top-to-the-north deformation is characterized by a single set of, approximately 20–30° north dipping extensional shear bands. Most of these shear bands are generally thick and clearly operate in the purely ductile regime. However, other shear bands show a continuum of shear from ductile to brittle regimes with an increasing localization within a precursory ductile; last increments of motions being operated under brittle conditions (Figure 9). Crosscutting relationships clearly indicate that top-to-the-south deformation systematically predates top-to-the-north deformation (Figure 9). These relations are additionally strengthened by the evolution toward a more brittle behavior of the top-to-the-north shear bands (Figure 9).

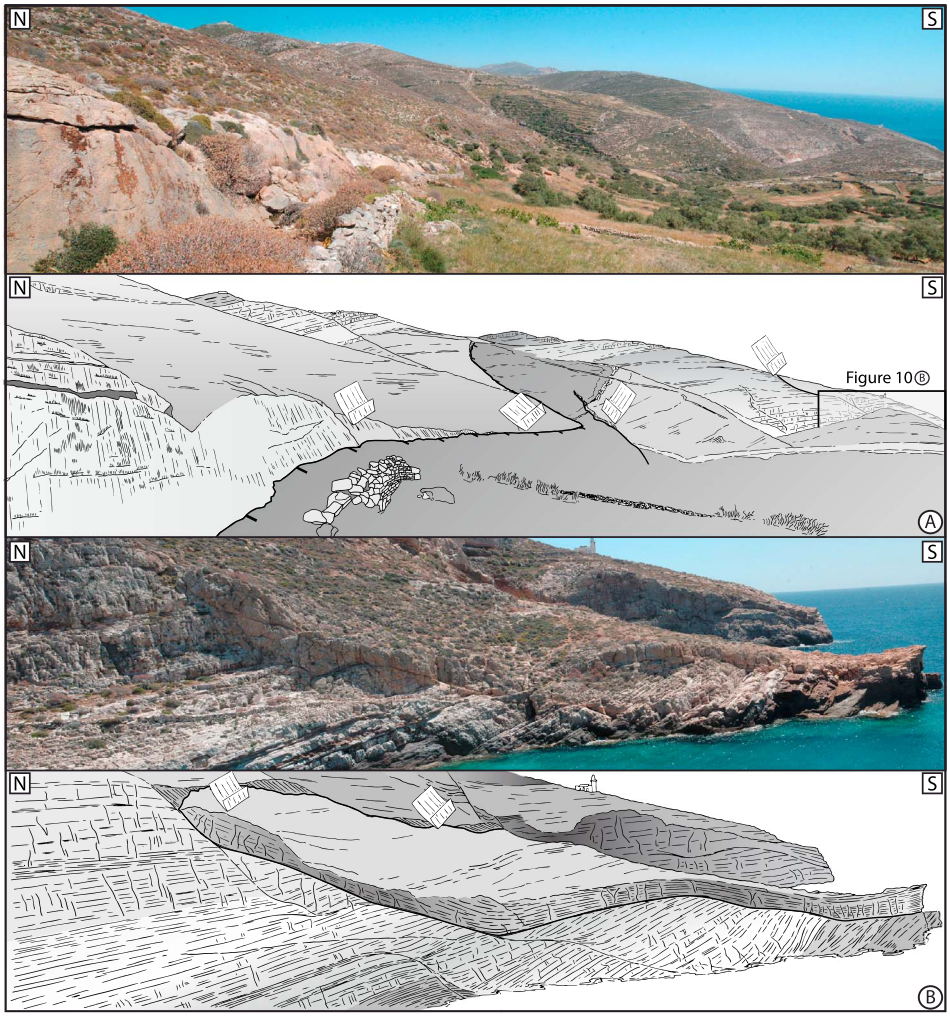

Figure 10. Mesoscale brittle structures. (a) Large-scale listric normal faults. (b) Flat-ramp-flat extensional system located approximately 1 km south of Figure 10a. Both outcrops show hanging wall displacements toward the south (Figure 4). Kinematics of mesoscale structures is consistent with the microscale brittle structures. See Figure 4 for location.

6. Analysis of Brittle Structures

6.1. Description of Brittle Structures

The whole study area presents a pervasive network of mesoscale to small-scale ductile-brittle shear zones and brittle faults systems developed from the ductile-brittle transition to the brittle field. Together with the Ambeli shear zone, the Cycladic Blueschists/Cycladic Basement contact are the only large-scale structures that were active under both ductile and subsequent brittle conditions and thus played a major role during the final exhumation stages of the Cycladic Basement unit. Displacement over the Cycladic Blueschists/Cycladic Basement contact is attested by the development of a thick zone of cataclasites reaching 15 m (Figure 9a). At map scale, kinematics of brittle motion over the Cycladic Blueschists/Cycladic Basement contact consistently indicates top-to-the-north motions (Figure 3). At the scale of the outcrop, kinematics of both the ductile and the brittle are similar (Figure 9b).

Mesoscale structures are heterogeneously distributed. They are particularly abundant on the southwestern part of Folegandros (Figure 4). The geometry of these faults seems clearly related to the strong lithologic (i.e., rheologic) layering of the metamorphic sequence (Figure 5). In the marble or quartzite layers, normal faults generally develop as 60–70° dipping roughly planar surfaces (Figure 10a). Conversely, metapelite layers are traversed by more gently dipping faults that sometimes reactivate low-angle shear zones. These two types of faults both oriented approximately west-east to NW-SE, interact, and often form flat-ramp-flat

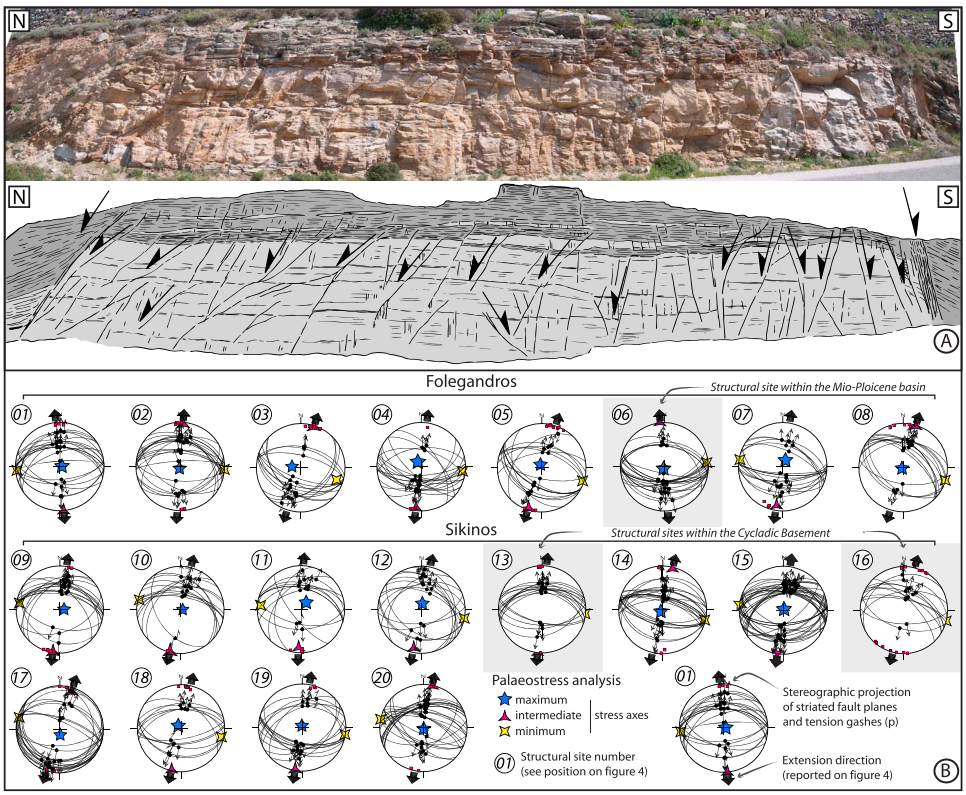

Figure 11. Small-scale brittle structures. (a) Representative outcrop recognized as demonstrative of a brittle stage subsequently developed after the ductile one (site 15; see location in Figure 4). Faults occur as a dense array of conjugate steep normal faults. (b) Detailed results of the fault slip data inversion (in the sense of *Angelier* [1994]). Note that the results present little internal dispersion and a marked consistency of the stretching direction (σ3, the minimum principal stress axis; see Figure 4 for comparison). Fault planes, associated striae, and results of inversion were plotted using the Tector software in Schmidt's lower hemisphere equal-area projection [*Angelier*, 1990]. Detailed results are given in Table 1.

systems or sets of listric normal faults that bend down on a layer-parallel gently dipping master normal fault (Figure 10). Displacement over mesoscale shear zones and faults are rarely constrained in the field but may routinely exceed tens of meters and the hanging wall is most often displaced toward the south (Figures 4 and 10).

Small-scale brittle structures mostly correspond to late approximately W-E conjugate normal faults systems. Displacement on faults ranges typically between few centimeters and few decimeters. However, in the entire studied area, the fault population is dominated by dihedral orientations arguing for the formation of newly formed conjugate sets of faults rather than the reactivation of former planes (Figure 11). Normal faults are often accompanied by a pervasive array of subvertical joints and tension gashes filled with calcite, quartz, chlorite, iron oxyhydroxides, or even barite in the Cycladic Basement (Figure 11b). Their close association often displays contradictory intersection relationships and thus argues for a contemporaneous development.

6.2. Inversion of Fault Slip Data: Methodology and Results

Paleostress orientation patterns were evaluated by the computer-aided inversion method for fault slip data, which is described in detail by *Angelier* [1984, 1990, 1994]. The reduced paleostress tensor consists in the identification of the orientation of the three principal stress axes (σ_1, σ_2, σ_3, the maximum, intermediate, and minimum stress axes, respectively), and the ratio $\Phi = [(\sigma_2 - \sigma_3)/(\sigma_1 - \sigma_3)]$ reflecting the axial ratio of stress ellipsoid. Determination of the paleostress axes has been completed by the analysis of other accompanying brittle structures such as joints, and tension gashes [*Hancock*, 1985]. The fault population used in this study is composed of microfaults populations embracing structures ranging from centimetric to decametric faults associated with cogenetic microfaults, which are observable on a single and continuous exposure.

Kinematics of mesoscale faults was not included in the paleostress reconstruction. Brittle structure analysis was conducted over 20 sites in all lithologies on both islands mainly in the Cycladic Blueschists Unit. Station 6 is located on the fault-bounded Miocene basin of Folegandros and stations 13 and 16 correspond to the Cycladic Basement Unit (Figure 11). Inversion of fault slip data was carried out using a representative number of measured striated fault, joints and tension gashes planes (451 in total) with a set of 15–25 faults routinely collected at each site. Results are all reported in Figure 11 and summarized in Figure 4. Orientations of the computed stress axes together with the values of the stress ellipsoid shape ratio Φ and estimators of the quality of the numerical calculation of the tensor are presented in Table 1.

Despite the local coexistence of both low angle and steep approximately N90–110°E trending normal faults highlighting possibly successive deformation increments, results present little internal dispersion. In all stations, the stress tensor analysis shows a consistent subvertical orientation for the maximum principal stress axis (σ_1) eliminating significant late horizontal axis rotations. The minimum principal stress axis (σ_3) is horizontal or gently plunging with a consistent N010°E direction since strikes range from N176°E to N016°E (Figure 11) preventing in turn for significant vertical axis rotations. Joint and tension gash planes correspond to the calculated σ_1-σ_2 plane, and their poles then appear scattered around the σ_3 axis. The ductile and the subsequent brittle structures recorded during the exhumation of both the Cycladic Blueschists Unit and the Cycladic Basement present a marked consistency of the stretching direction across the ductile-brittle transition.

7. Quantitative P-T Constraints

7.1. Sampling Strategy

Additionally, to the cartographic qualitative distribution of index minerals (Figure 6) and recent P-T estimates for the Cycladic Basement unit [e.g., *Gupta and Bickle*, 2004; *Huet*, 2010], peak-metamorphic conditions were quantitatively explored in the Cycladic Blueschists unit on Sikinos and Folegandros. Two independent methods were used: average P-T calculations using THERMOCALC [*Holland and Powell*, 1998] and maximum temperatures using Raman Spectroscopy of Carbonaceous Material (RSCM) [*Beyssac et al*., 2002, 2003]. Being poor in metamorphic minerals and often heavily retrograded into greenschist-facies conditions (Figure 6), rocks from Folegandros were not used for the average P-T approach. P-T calculations then focused on metamorphic rocks from Sikinos and were conducted on four rock samples from protoliths of contrasted compositions. To gather a representative data set for the RSCM approach, 25 carbonaceous material (CM)-rich metasedimentary rocks were collected across the metamorphic succession of both islands including the Cycladic Basement Unit. Analytical techniques used herein are presented in details in the supporting information; reader unfamiliar with THERMOCALC or the RSCM approaches is referred to recent publications [*Beyssac et al*., 2002; *Augier et al*., 2005c; *Plunder et al*., 2012]. Peak-equilibrium conditions and independent RSCM peak-T results that have been investigated for the first time on these islands are presented below.

7.2. P-T Results

For the sake of brevity, samples involved in the average P-T thermobarometric calculations are all described in details in the supporting information addressing briefly outcrop conditions, mineral habits, phase relationships, and detailed mineral compositions. Representative Electron-Probe Micro-Analyses (EPMA) of the minerals involved in peak conditions parageneses are also presented in a supporting information. Mineral abbreviations used in this work are after *Whitney and Evans* [2010]. Average P-T calculations were focused on metapelite, metabasite rock samples, and rocks of intermediate compositions such as glaucophane-(chloritoid) micaschists.

Rocks of intermediate compositions are abundant on Sikinos, while only some rare occurrences crop out on Folegandros (Figure 6). Depending on the relative modal proportion of the rock-forming minerals, rocks may appear as blue-amphibole micaschists (Sik09006) or as micaceous "glaucophanites" (Sik09002). These rocks generally occur as rather continuous 3 to up to 10 m thick layers. Their mineralogy generally comprises in order of decreasing abundance gln + ph + grt + qz + pg + rt + chl ± ctd. These rocks present more locally a glaucophane-chloritoid association which highlights a peculiar protolith chemistry and a mineral association characterized by a narrow stability field at approximately 480–550°C for some 17–25 kbar [e.g., *Wei and Powell*, 2004] discarding previous P-T results performed on Sikinos [*Gupta*, 1995].

AGU Tectonics

10.1002/2014TC003664

Table 1. Detailed Results of the Paleostress Analysis[a]

Location Station	Location (GPS Position)		General Information				Calculated Results									
					MF/S0 Attitude				S1		S2		S3		RUP	
	X	*Y*	Tectonic Unit	Dominant Lithology	Dir.	Plung.	*N*	Joints	Dir.	Plung.	Dir.	Plung.	Dir.	Plung.	(%)	Phy
						Folegandros										
1	36°39,052	24°50,643	Cycladic Blueschists	Metapelites	004	26	20	3	081	86	265	04	175	00	19	0.4
2	36°39,867	24°51,383	Cycladic Blueschists	Metapelites	021	21	21	8	200	86	094	01	004	04	17	0.6
3	36°38,855	24°52,407	Cycladic Blueschists	Marbles/metapelites	048	23	17	8	278	74	108	16	018	03	23	0.7
4	36°38,485	24°53,701	Cycladic Blueschists	Marbles/metapelites	63	25	19	5	320	81	102	03	187	04	23	0.7
5	36°37,784	24°53,702	Cycladic Blueschists	Metapelites/marbles	72	23	15	11	339	84	108	04	198	05	19	0.6
6	36°37,648	24°55,047	Sedimentary basin	Limestones	198	60	18	6	169	89	082	04	355	02	18	0.5
7	36°37,353	24°55,972	Cycladic Blueschists	Marbles	42	12	15	3	042	82	282	02	192	07	15	0.5
8	36°36,333	24°57,218	Cycladic Blueschists	Metapelites	062	23	15	6	235	87	107	02	017	02	09	0.5
9	36°37,421	25°00,554	Cycladic Blueschists	Marbles/metapelites	259	26	17	8	086	82	279	08	189	02	18	0.6
						Sikinos										
10	36°37,952	25°01,560	Cycladic Blueschists	Marbles	265	19	16	3	081	86	284	04	194	02	23	0.7
11	36°38,157	25°04,568	Cycladic Blueschists	Marbles/metapelites	325	17	16	4	038	74	275	09	183	13	24	0.4
12	36°39,656	25°05,132	Cycladic Blueschists	Marbles/metapelites	032	21	15	10	008	78	101	01	191	12	24	0.5
13	36°38,795	25°05,771	Cycladic Basement	Metapelites	345	06	17	9	311	88	096	02	186	01	12	0.4
14	36°40,426	25°05,775	Cycladic Blueschists	Metapelites/marbles	006	19	24	7	228	86	103	02	013	04	22	0.5
15	36°41,262	25°06,133	Cycladic Blueschists	Metapelites/marbles	182	12	10	4	062	88	280	02	190	01	23	0.7
16	36°39,529	25°07,519	Cycladic Basement	Granodiorite	018	23	12	15	198	86	104	00	014	04	23	0,4
17	36°40,454	25°08,794	Cycladic Blueschists	Marbles	054	15	24	5	175	79	287	04	017	10	32	0.7
18	36°42,396	25°08,931	Cycladic Blueschists	Marbles	042	12	15	7	312	83	102	06	193	03	13	0,4
19	36°41,676	25°08,680	Cycladic Blueschists	Marbles/metapelites	046	18	18	3	349	86	099	01	189	03	15	0,6
20	36°41,539	25°09,960	Cycladic Blueschists	Marbles/metapelites	048	06	23	5	161	88	282	01	012	01	20	0,5
						Total	321	130								

[a]Indicated are, after a brief description of the site (tectonic unit, dominant lithology, and foliation/bedding attitude), the composition of the data set and results of the paleostress tensor determination. Results consist in the orientation of the three principal stress axes (σ_1, σ_2, σ_3, the maximum, intermediate, and minimum stress axes, respectively), the RUP value which is a quality estimator and the Phy ratio = $[(\sigma_2 - \sigma_3)/(\sigma_1 - \sigma_3)]$ reflecting the relative magnitude of principal stress axes (axial ratio of stress ellipsoid).

Average P-T thermobarometric calculations were performed to put new constraints on the Cycladic Blueschists unit in the Southern Cyclades. Average P-T results are presented in Table 2. For each sample, several runs were made using coexisting mineral compositions considered to reflect equilibrium associations at peak conditions. End-members presenting very small activities compared to the associated uncertainties were routinely removed. Relying on output statistical parameters (i.e., *e** and hat) [*Holland and Powell*, 1998], amesite end-members were often also removed, suggesting a possible partial reequilibration of chlorite. Models for chlorite activities are indeed currently discussed [*Angiboust et al.*, 2011]. Calculated average P-T conditions for peak assemblages are fairly homogeneous and span a range between approximately 490 and 530°C for 18–20 kbar (Figure 12a). Peak-equilibrium conditions of 512 ± 11°C and 19.3 ± 1.2 kbar were obtained on the assemblage Gln-Grt-Ph-Cld-Chl-Ep-Rt-Qz-H_2O [a(H2O) = 1, cor = −0.033, sigfit = 1.08/1.41] in the glaucophane-chloritoid-micaschists appearing as the most constraining assemblages (sample Sik09006, Figure 12a). Similar conditions (509 ± 35°C and 18.7 ± 3.2 kbar but with larger error bars were derived from Gln-Grt-Ph-Chl-Ep-Rt-Qz-H_2O) [a(H2O) = 1, cor = −0.894, sigfit = 0.9/1.54] in the glaucophane-micaschists (sample Sik09002, Figure 12b). Grt-Ph-Cld-Chl-Cal-Qz-H_2O assemblage [a(H2O) = 1, cor = −0.170, sigfit = 0.32/1.65] in the metapelite sample (sample Sik266-11, Figure 12c) yielded 493 ± 11°C and 18.7 ± 1.3 kbar, while the Omp-Ph-Grt-Rt-Qz-H_2O assemblage in the metabasite sample (sample Sik295-11, Figure 12d) yielded 528 ± 52°C and 18.9 ± 2.4 kbar. In the absence of study dealing with fluid inclusions trapped in HP minerals, calculations were routinely conducted with a(H2O) = 1. Sensitivity of the results to water activity changes were evaluated for decreasing water activities. Decrease of a(H2O) from 1 to 0.8 or from 0.8 to 0.6 only induces that temperature is generally only lowered by 10–20°C while effect on pressure is negligible (approximately 0.1 to 0.4 kbar). Conversely, effects of increasing CO_2 activity (aCO_2) are drastically more important for the metapelite sample Sik11266 where carbonates were observed. P-T equilibrium conditions are shifted down to approximately 16.5 kbar for 530°C for $aCO_2 = 0.1$ or to approximately 15.5 kbar for 512°C for $aCO_2 = 0.2$ with approximately 3.5 to 5 kbar uncertainties (Table 2).

7.3. RSCM Tmax Results

Average P-T results were complemented by independent peak-temperature estimates. The data set consists of 25 CM-bearing samples collected in metapelite layers regularly distributed within the islands of Sikinos (12 samples) and Folegandros (13 samples). RSCM temperatures are reported in Figures 6 and 12b and in the Table 3. Detailed results, including R2 ratio, number of spectra, Tmax, and standard deviation are presented in ascending structural order in Table 3. Twenty to twenty-five spectra were routinely recorded for each sample to bring out and possibly smooth out the inner structural heterogeneity of CM within samples. Internal dispersion of RSCM Tmax presents generally unimodal Tmax distributions and ranges from 7 to 23°C (Table 3). Conversely, samples from the Cycladic Blueschists unit on Sikinos display higher dispersions ranging from 25 to 34°C possibly in response to the presence of an inherited component of CM [*Beyssac et al.*, 2002]. Inheritance was detected within six samples by bimodal RSCM Tmax distribution sharing a common 580–600°C well-defined peak. The contribution of this HT component was thus removed for RSCM Tmax calculations. Spectra were then processed using the software Peakfit as described in *Beyssac et al.* [2002] or *Lahfid et al.* [2010]. RSCM temperatures embrace a wide range of temperature from 321 to 622°C and drastically contrast from Sikinos to Folegandros with a minimum of 80°C of difference; RSCM results are thus discussed separately (Figure 12e).

Two main sets of RSCM temperatures can be identified on Sikinos from Figure 12b: rather high, approximately 600°C temperatures for the Cycladic Basement unit and lower temperatures for the Cycladic Blueschists unit. Samples from the metasedimentary layers from the Cycladic Basement show average Tmax ranging from 580 to 620°C; all consistent with prealpine amphibolite-facies conditions [e.g., *van der Maar*, 1980, *van der Maar et al.*, 1981; *Franz et al.*, 1993]. Two samples yielded approximately 580°C and a slightly higher Tmax (i.e., 622°C) was even obtained from a third sample picked in the vicinity of the largest granitoid body (Figure 12e). Rocks from the Cycladic Blueschists unit all display lower temperatures, falling between 500 and 540°C that match, in a broad sense, the temperatures derived from the average P-T approach. Samples from the structurally deeper part of the metamorphic succession show consistent average RSCM Tmax ranging from 547 to 526°C. Slightly lower temperatures of approximately 500°C were obtained for the higher parts of the metamorphic succession (samples Sik11182 and Sik11194), structurally above the Voudhia Shear zone. Interestingly, Tmax ascribed to an inherited HT component all fall between 578 and 599°C and thus yield similar temperatures as those obtained for the Cycladic Basement rocks.

AGU Tectonics

Table 2. Detailed Results of the THERMOCALC Average P-T Estimates[a]

Location Sample	Location (GPS Position)		Sample Description		Average P-T Results								
	X	*Y*	Metamorphic Sequence	Paragenesis	P/DP (kbar)	SP (kbar)	T/DT (°C)	ST (°C)	Corr./Dcorr.	Sigfit./Dsigfit	Th. Sigfit	N React.	N Calc.
Sik09006	36°41,680	25°07,587	Intermediate	Grt-Gln-Cld-Chl-Ph-Ep-Ru-Cal-Qz (aH2O = 1)	19,3 ± 0,6	1,3 ± 0,2	514 ± 9	11 ± 3	−0,033 ± 0,008	1,08 ± 0,17	1.41	8	8
				Grt-Gln-Cld-Chl-Ph-Ep-Ru-Cal-Qz (aH2O = 0,8)	18.7	1.5	499	16	−0.034	1.12	1.41	8	1
Sik09002	36°41,611	25°07,639	Intermediate	Grt-Gln-Chl-Ph-Ep-Ru-Qz (aH2O = 1)	18,7 ± 0,7	3,3 ± 0,1	515 ± 17	35 ± 3	−0,891 ± 0,009	0,87 ± 0,09	1.54	6	10
				Grt-Gln-Chl-Ph-Ep-Ru-Qz (aH2O = 0,8)	18.4	3.1	484	32	−0,898	0.82	1.54	6	1
Sik11266	36°41,634	25°10,036	Metapelite	Grt-Cld-Chl-Ph-Qz (aH2O = 1)	19,1 ± 0,6	1,4 ± 0,2	496 ± 12	14 ± 6	−0,175 ± 0,054	0,65 ± 0,34	1.61	5	9
				Grt-Cld-Chl-Ph-Qz (aH2O = 0,8)	18.5	1.5	484	16	−0.135	0.76	1.61	5	1
				Grt-Cld-Chl-Ph-Qz (aH2O = 0,6)	18.3	1.8	476	18	−0.123	0.96	1.61	5	1
				Grt-Cld-Chl-Ph-Qz-Cal (aH2O = 0,9; aCO2 = 0,1)	15.5	3.5	530	34	0.369	1.24	1.54	6	1
				Grt-Cld-Chl-Ph-Qz-Cal (aH2O = 0,8; aCO2 = 0,2)	16.5	4.9	512	29	0.325	1.17	1.54	6	1
Sik11295	36°41,739	25°10,255	Metabasite	Grt-Omph-Ph-Ru-Qz- (aH2O = 1)	19,1 ± 0,4	2,4 ± 0,2	530 ± 12	51 ± 4	−0,375 ± 0,026	0,46 ± 0,15	1.96	3	9
				Grt-Omph-Ph-Ru-Qz- (aH2O = 0,8)	18.5	2.5	510	50	−0,348	0.3	1.96	3	1

[a]Indicated are the peak conditions mineral association and the detailed results of the calculations for four samples of contrasted bulk chemical composition. Accuracy of the P-T estimates is typically of the order of 1–2 kbar for pressure and of 10–30°C for temperature. According to *Powell and Holland* [1994], DP and DT corresponds respectively to the range of variation in pressure and in temperature. SP and SD corresponds respectively to the the mean values of the output error on pressure and temperature. Corr. corresponds to the orientation of the long axis of the error ellipse. Sigfit is a posttreatment equilibrium test criteria that must be compared to th. Sigfit which is the theoretical cutoff value. N React. is the number of independent reactions, and N Calc. is the number of THERMOCALC calculations (i.e., runs) with different sets of minerals. Also presented are results on the dependency of the P-T estimates for different H_2O and CO_2 activities.

10.1002/2014TC003664

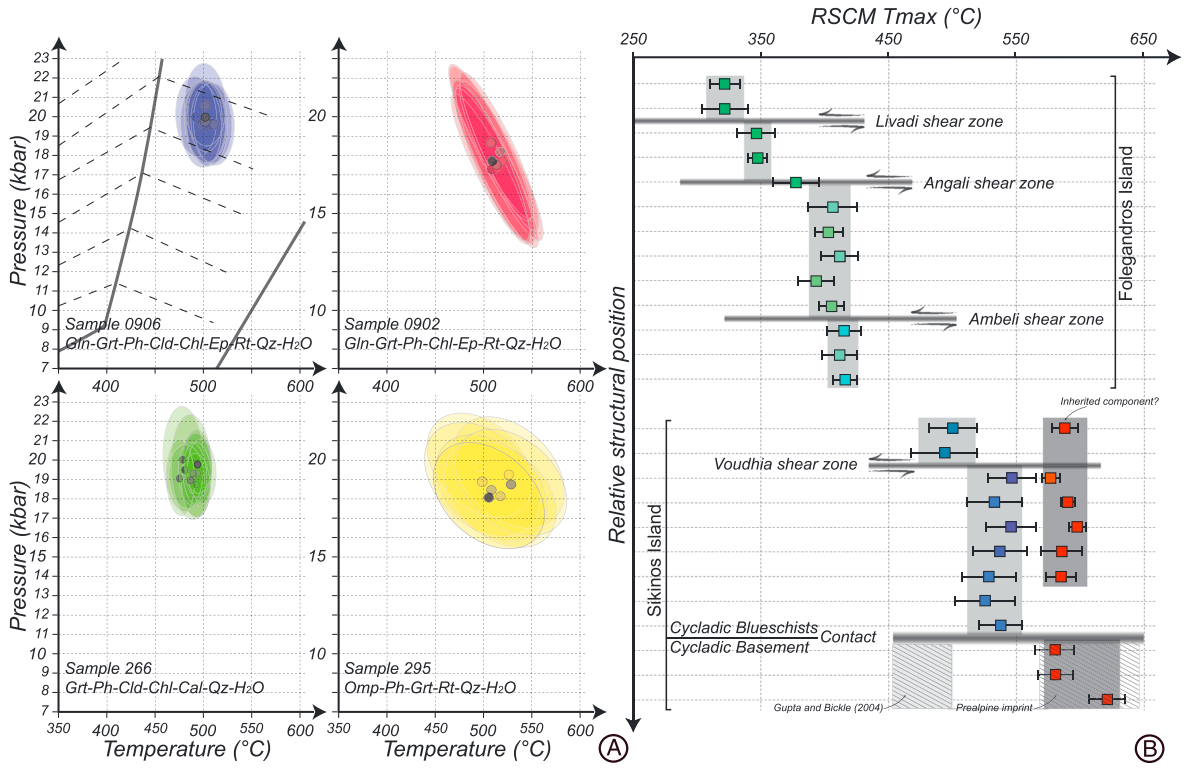

Figure 12. P-T constraints. (a) Average P-T results presented for the four samples. For the sake of clarity, P-T points and related error bars are shown only for the runs performed for H_2O activity = 1. Error brackets are based on the 1 s uncertainties on pressure and temperature results. (b) RSCM peak temperature results versus structural relative position in the metamorphic succession. Indicated is the position of the main shear zones deduced form the structural approach. Error brackets correspond to intrasample heterogeneity.

Rocks from the Cycladic Blueschists unit from Folegandros display much lower temperatures, falling between 415 and 320°C (Figure 12b). RSCM Temperatures appear quite homogeneous at around approximately 415–395°C in the lower part of the structure were HP rocks including blue-amphibole and lawsonite rocks occur. Conversely, the upper part of the metamorphic series is characterized by an approximately 80–100°C, decreasing stepwise toward the top of metamorphic succession in the SE of the island (Figure 12b). There, consistent Tmax as cold as approximately 320°C was thus obtained. The two main steps in the temperature profile correspond, in a broad sense, to the position of highly retrograded high-strain zones detected during the field survey (i.e., the Livadi and the Angali shear zones). Conversely, the deeper Ambeli shear zone does not correspond to a significant temperature change.

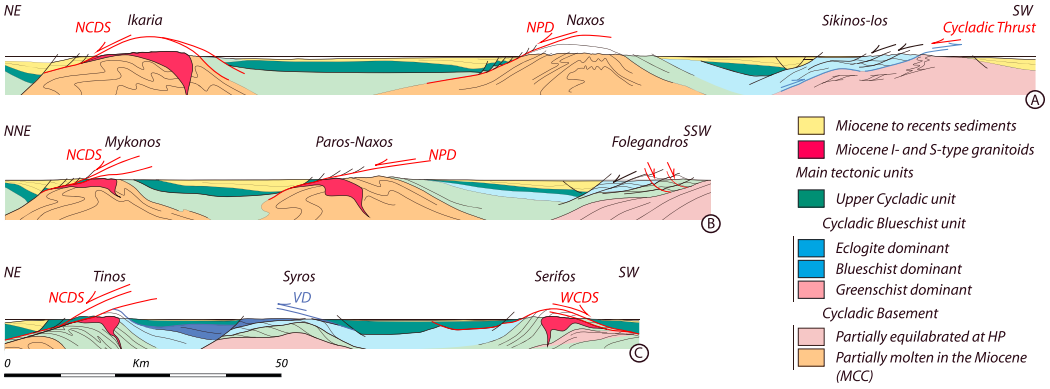

Figure 13. (a–c) Cross sections through the Cycladic archipelago. Sections are all roughly parallel to the tectonic transport and allow highlighting the increasing amount of stretching to the center of the Aegean domain. See Figure 1 for location.

Table 3. RSCM Tmax Results[a]

Location Sample	Location (GPS Position)		Tmax Detailed Results							
				Temperature				Inherited Component (If Detected)		
	X	*Y*	Total Number of Spectra	Mean R2	Tmax	SD	*n*	*T*	SD	*n*
				Folegandros						
Fol002-13	36°36,129	24°57,089	19	0.72	321	12	17			
Fol001-13	36°36,337	24°57,246	17	0.72	321	18	16			
Fol019-13	36°36,927	24°57,043	23	0.66	346	14	22			
Fol004-13	36°36,184	24°56,284	20	0.66	347	7	20			
Fol003-13	36°37,940	24°54,166	20	0.59	377	18	18			
Fol018-13	36°36,392	24°54,396	17	0.53	406	19	17			
Fol009-13	36°39,369	24°50,684	20	0.54	402	11	20			
Fol013-13	36°37,827	24°53,439	23	0.52	411	14	22			
Fol012-13	36°38,709	24°51,686	20	0.56	393	14	20			
Fol006-13	36°39,039	24°50,679	20	0.53	405	10	20			
Fol007-13	36°38,738	24°51,048	20	0.51	415	13	20			
Fol016-13	36°38,211	24°52,393	20	0.52	411	14	20			
Fol014-13	36°37,788	24°52,668	20	0.51	416	9	20			
				Sikinos						
Sik193-11	36°42,786	25°10,218	29	0.32	500	19	19	589	10	10
Sik182-11	36°42,360	25°10,424	18	0.33	494	26	17			
Sik208-11	36°42,436	25°09,056	21	0.21	547	18	16	578	7	5
Sik293-11	36°41,484	25°07,900	20	0.24	533	21	15	592	6	5
Sik294-11	36°42,005	25°07,212	27	0.21	546	19	14	599	6	13
Sik078-11	36°40,188	25°05,640	29	0.23	537	20	24	586	15	5
Sik215-11	36°40,767	25°07,868	21	0.25	528	19	15	587	12	6
Sik290-11	36°39,616	25°04,964	22	0.26	526	23	22			
Sik214-11	36°40,168	25°07,817	20	0.23	538	17	18			
Sik102-11	36°38,423	25°04,606	28	0.14	580	14	25			
Sik512-11	36°38,758	25°05,646	22	0.13	581	13	21			
Sik284-11	36°39,544	25°07,284	18	0.04	622	14	18			
					Total		459	Total		44

[a]Indicated are the total number of Raman spectra performed on the sample, the mean R2 ratio, the RSCM temperature, and the uncertainty related to the intrasample heterogeneity. In the calculation of the Tmax, *n* corresponds to the effective number of spectra involved. Another temperature was calculated for samples that present an inherited HT component.
See location of the samples and results in Figure 6.

8. Interpretations and Discussion

8.1. An Overall Top-to-the-North Asymmetry During the Exhumation of the Southern Cyclades

The entire metamorphic series of the Cycladic Blueschists unit on Sikinos and Folegandros, exposed as a north to NE dipping monocline, is pervasively affected by top-to-the-north deformation (Figures 4 and 8). Besides, top-to-the-north deformation exhibits strain gradients toward the north in the vicinity of a series of extensional shear zones where deformation is further localized (Figures 2 and 8). Four main extensional shear zones were recognized and documented within the Cycladic Blueschists unit: from bottom to top of the structure, the Voudhia shear zone on Sikinos and the Ambeli, Angali, and Livadi shear zones on Folegandros (Figure 2). Top-to-the-north deformation is also heavily concentrated along the Cycladic Blueschists/Cycladic Basement contact that is marked by an approximately 200 m thick mylonite zone developed at the expense of the Cycladic Basement rocks (Figure 9). All these strain gradients are accompanied by coeval retrogression gradients in greenschist-facies conditions able to completely erase the former HP/LT imprint in the core of the shear zones (Figure 8). Correlations at all scales between gradient of noncoaxial strain and gradient of retrogression are interpreted as the expression of progressive localization allowing the final exhumation of both the Cycladic Blueschists and the Cycladic Basement units and, conversely, promoting the preservation of earlier tectonometamorphic features in less deformed areas (Figure 6). The Cycladic Blueschists/Cycladic Basement contact and the Ambeli shear zone also recorded late increments of motions in brittle conditions with the development of thick cataclasite zones (Figure 8). This evolution, also

recognized on Andros [e.g., *Mehl et al*., 2007], Tinos [e.g., *Mehl et al*., 2005], Mykonos [e.g., *Lecomte et al*., 2010], or Serifos [e.g., *Grasemann and Petrakakis*, 2007] is interpreted as an evidence of continuous stretching and shearing from middle-to-upper crustal levels, from ductile to brittle regime. Furthermore, inversion of fault slip data shows that ductile and the subsequent brittle structures recorded during the exhumation of the Cycladic Blueschists and the Cycladic Basement units present a marked consistency of the stretching direction indicating an approximately north-south strain continuum through the ductile-brittle transition (Figure 4). Inversion of fault slip data collected within and far away from the detachment zone also shows that the maximum principal stress axis remained subvertical during brittle deformation throughout the islands as suggested by the vertical orientation of the veins (Figure 11). The high angle of the maximum principal stress axis to the detachment "planes" suggests that detachments were active at very shallow dip angle and were therefore weak fault zones as already the demonstrated for both the NCDS and the WCDS on Tinos, Mykonos, or Serifos [*Mehl et al*., 2005, 2007; *Lecomte et al*., 2010; *Grasemann et al*., 2012]. The final exhumation across the brittle-ductile transition is thus dominantly associated with asymmetric extension dominated by top-to-the-north deformation as already proposed for Ios [*Huet et al*., 2009]. On this island, low-temperature geochronology pointed out an apparent northward younging of zircon FT (14.5 ± 1.6 to 13.5 ± 1.4 Ma), apatite FT (12.2 ± 1.4 to 11.0 ± 1.4 Ma), and apatite U-Th/He ages (10.8 ± 1.0 to 9.5 ± 0.8 Ma) in the Cycladic Basement unit consistent with an overall top-to-the-north unroofing [*Brichau*, 2004]. This northward younging therefore implies that the formation of the Ios dome postdates the activity of the Cycladic Blueschists/Cycladic Basement contact. While some domes are interpreted "a-type" MCC [*Jolivet et al*., 2004] formed at depth during north-south stretching at circa 20–18 Ma [e.g., *Gautier et al*., 1993; *Keay et al*., 2001; *Jolivet et al*., 2004; *Vanderhaeghe*, 2004; *Duchêne et al*., 2006; *Martin et al*., 2006], some others may correspond to large-scale late folds [e.g., *Avigad et al*., 2001]. Description of small to large-scale open folds, strike-slip faults, or even minor thrusts in the Northern Cyclades, the northern Dodecanese, and western Turkey suggested the existence of an approximately E-W compressional regime [*Angelier*, 1976; *Buick*, 1991; *Bozkurt and Park*, 1997; *Ring et al*., 1999; *Avigad et al*., 2001; *Bozkurt*, 2003] active since 9–8 Ma [*Weidmann et al*., 1984; *Ring et al*., 1999; *Menant et al*., 2013]. Although this event is not recorded by brittle structures, it appears, however, tempting to propose that the arching of the ductile to brittle fabrics over Sikinos are related to a late significant component of E-W shortening.

8.2. Importance of the Top-to-the-North Intra-Cycladic Blueschists Shear Zones

The Cycladic Blueschists unit that crops out on Sikinos and Folegandros is affected by a set of top-to-the-north extensional shear zones that allow separating subunits. By nature, intra-Cycladic Blueschists shear zones cannot be compared to first-order detachments as observed on Tinos [e.g., *Patriat and Jolivet*, 1998; *Mehl et al*., 2005] or Mykonos [e.g., *Lecomte et al*., 2010; *Denèle et al*., 2011; *Menant et al*., 2013] along the NCDS or on Kea, Kithnos, and Serifos [e.g., *Grasemann and Petrakakis*, 2007; *Iglseder et al*., 2009, 2011; *Tschegg and Grasemann*, 2009; *Schneider et al*., 2011; *Grasemann et al*., 2012] along the WCDS as these structures separate the Cycladic Blueschists unit from Pelagonian or even sedimentary units. Each of these detachments is characterized by a single yet major normal-sense metamorphic gap. For example, the Tinos detachment juxtaposes large portions of Cycladic Blueschists equilibrated homogeneously at approximately 18–20 kbar for 530°C [*Parra et al*., 2002; *Beyssac et al*., 2002] against the nonmetamorphosed Pelagonian unit on Tinos. In the Southern Cyclades, this type of structure has not been observed, neither on the studied islands nor on Ios [*Forster and Lister*, 1999a; *Huet et al*., 2009]. On the contrary, a major result of this study is the recognition of a set of top-to-the-north extensional shear zones that dismembers the initial (i.e., synorogenic) thermal structure of the Cycladic Blueschists unit during postorogenic extension in subunits of contrasted peak-T (and probably peak-P) conditions. RSCM results thus showed a stepwise decrease of more than 200°C within the Cycladic Blueschists unit from approximately 530°C at the base to approximately 320°C toward the top of the metamorphic series. As graphitization is an irreversible transformation, RSCM temperatures discard retrogression effects. Importantly, only the lower subunit of the Cycladic Blueschists unit yielded approximately 18–20 kbar for 530°C peak conditions in the Southern Cyclades. It is therefore proposed that all the upper subunits with intermediate temperatures are tectonically omitted in the Northern Cyclades in the footwall of the NCDS. Conversely, the lower subunit, below the Voudhia shear zone would correlate with the Cycladic Blueschists units located just below the Tinos detachment on Tinos [*Jolivet et al*., 2010]. These new, postorogenic subdivisions of the Cycladic Blueschists unit add with synorogenic ones individualized on the basis of the degree of retrogression of HP assemblages during exhumation [*Trotet et al*., 2001a, 2001b; *Keiter et al*., 2004]. In this case, after an equilibration

in the eclogite-facies at conditions of approximately 18–20 kbar for 500–550°C, subunits experienced different exhumation histories coeval with convergent boundary conditions as recorded by continuous retrograde P-T paths including contrasted incursions through the greenschist-facies conditions [*Trotet et al*., 2001a, 2001b; *Groppo et al*., 2009].

8.3. The Southeastern Termination of the West Cycladic Detachment System

During the last few years, consistent top-to-the-south to -SW deformations were described on the Western Cyclades [*Grasemann and Petrakakis*, 2007; *Iglseder et al*., 2009, 2011; *Tschegg and Grasemann*, 2009; *Brichau et al*., 2010; *Schneider et al*., 2011]. Just as along the NCDS, a set of detachments separates the Cycladic Blueschists unit from a nonmetamorphosed upper unit of Pelagonian or a sedimentary affinity [e.g., *Sánchez-Gómez et al*., 2002; *Jolivet et al*., 2010] through a mylonitic and/or cataclastic zones (Figure 13). Based on a similar tectonometamorphic evolution in exhuming the Cycladic Blueschists and relying on consistent absolute time constraints, a mechanical link of these detachments as a single crustal-scale WCDS was recently proposed [*Grasemann et al*., 2012]. With a maximum displacement on Kea [*Iglseder et al*., 2011; *Grasemann et al*., 2012], the amount of ductile displacement decreases toward Attica in continental Greece, to the NW [*Krohe et al*., 2010] and toward Serifos, to the SE [*Grasemann and Petrakakis*, 2007]. For example, mylonites, strongly reworked in a polyphased cataclastic body reach only a few meters in thickness on Serifos [*Grasemann and Petrakakis*, 2007] limiting the extension of the WCDS to the SE of Serifos. The brittle top-to-the-south to -SSW deformation visible on Sifnos, mainly consisting in a low-angle normal fault system [*Ring et al*., 2011] was first proposed as a deformation related with and partly coeval to the WCDS [*Ring et al*., 2011; *Grasemann et al*., 2012]. In the lights of the structural observations of this study, it is proposed that the dense array of mesoscale top-to-the-south listric normal fault located in the SW of Folegandros would represent the southeasternmost witnesses of the deformation related to the WCDS (Figure 13). This result, together with the clear anteriority of the top-to-the-south with respect to the top-to-the-north deformation along the Cycladic Blueschists/Cycladic Basement contact as already shown by *Huet et al*. [2009] argues against the recent proposition of *Ring et al*. [2011] to merge the WCDS with the South Cycladic shear zone in the sense of *Lister et al*. [1984]. Conversely, the reactivation of the South Cycladic thrust as an top-to-the-north extensional shear zone shows that the top-to-the-north shear sense characterizing the NCDS extends all over the Southern Cyclades with common timing, kinematics, and tectonometamorphic evolution, in a broad sense. Just as the NCDS, which has been proposed to reactivate the Vardar suture zone [e.g., *Jolivet et al*., 2010], the extensional reactivation of the South Cycladic thrust shows that reactivation of earlier shallow-dipping discontinuities plays a first-order role in postorogenic extension (Figure 13).

8.4. Evolution of the Cycladic Blueschists/Cycladic Basement Contact

Despite a strong overprint by top-to-the-north ductile and later brittle deformation, the detailed field survey reported in this study shows that the contact between the Cycladic Blueschists unit and the Cycladic Continental Basement unit was initially associated with top-to-the-south movements (Figure 9). These observations confirm the general kinematics observed on Ios as proposed by previous authors [*Lister et al*., 1984; *Vandenberg and Lister*, 1996; *Forster and Lister*, 1999a; *Huet et al*., 2009]. More importantly, these observations reinforce the polyphased character of the Cycladic Blueschists/Cycladic Basement contact showing that top-to-the-south displacements clearly predate top-to-the-north deformation prevailing during the final exhumation stages of both the Cycladic Blueschists and the Cycladic Basement units just as on Ios [*Huet et al*., 2009]. There, it has been recently demonstrated that top-to-the-south deformation recorded either within the Cycladic Blueschists and Cycladic Basement units or along the Cycladic Blueschists/Cycladic Basement contact (i.e., the South Cycladic shear zone [e.g., from *Lister et al*., 1984 to *Ring et al*., 2011]) was associated with thrust tectonics (i.e., the South Cycladic thrust; [*Huet et al*., 2009]), active under HP-LT conditions [*Huet et al*., 2009]. Classically interpreted as the evidence of exhumation in the subduction zone, synkinematic retrogression of eclogite in blueschist-facies conditions has been already described on Syros and Sifnos Islands where top-to-the-NE synorogenic detachments are preserved from subsequent reworking [*Trotet et al*., 2001a, 2001b; *Jolivet et al*., 2004]. Thus, the Cycladic Blueschists unit was limited by a top-to-the-south basal thrust and a top-to-the-NE detachment at its top defining an extrusion structure that operated in the subduction zone during the Eocene [*van der Maar and Jansen*, 1983; *Baldwin*, 1996; *Baldwin and Lister*, 1998; *Ring et al*., 2007a, 2007b; *Huet et al*., 2009; *Jolivet and Brun*, 2010; *Huet*, 2010]. Initially estimated to only 11 kbar for 475°C [*Gupta and Bickle*, 2004; *Thomson et al*., 2009], peak P-T conditions of the

Cycladic Basement unit were reviewed and corrected to 16.5 ± 1.3 kbar for 500 ± 20°C by pseudosection modeling on Ios [*Huet*, 2010]. These new results fall in the same range of P-T conditions retrieved for the basal subunit of the Cycladic Blueschists unit peak conditions on Sikinos at approximately 18.5 ± 1 kbar for 510 ± 20°C in this study or on Ios by similar pseudosection modeling on Ios at approximately 18.5 ± 1.3 kbar for 510 ± 20°C. The Cycladic Blueschists/Cycladic Basement contact appears therefore characterized by a weak yet inverse pressure gap that still argues for thrust motions despite a strong extensional overprint.

8.5. New Constraints on the Cycladic Blueschists Accretionary Wedge

Together with Oman or New Caledonia [*Agard and Vitale-Brovarone*, 2013], the Aegean domain and particularly the Cycladic Blueschists unit and therefore particularly the basal subunit is a world reference for HP-LT rock preservation where subduction-related processes are still observable. As these fossilized subduction complexes, the Cycladic Blueschists unit exposes exhumed tectonic units of subducted HP-LT continental material and/or transitional oceanic remnants of the Pindos basin [e.g., *Bonneau et al*., 1980; *Ring et al*., 2007a, 2007b; *Huet et al*., 2009] that were not modified by later collision and not all affected by the Oligo-Miocene thermal imprint [*Lister et al*., 1984; *Buick and Holland*, 1989; *Keay et al*., 2001; *Vanderhaeghe*, 2004; *Duchêne et al*., 2006; *Martin et al*., 2006]. Despite a strong greenschist overprint, analysis of HP-LT remnants (Figures 6 and 7a) rocks from Sikinos show that lawsonite-blueschists (Figure 7g) are turned into phengite-garnet-omphacite-bearing eclogite close to peak-burial conditions before recording an incipient retrogression in the epidote-blueschist-facies during the first exhumation step (Figure 7b). This mineralogical evolution, which is typical for subduction-related terranes, is also recorded in the neighboring islands of Ios [*Forster and Lister*, 1999a; *Huet et al*., 2009], Syros [*Trotet et al*., 2001a; *Schumacher et al*., 2008], or Sifnos [*Groppo et al*., 2009]. Estimation of peak-metamorphic conditions from rocks of contrasted chemical (and mineralogical) compositions throughout the island of Sikinos yielded fairly homogeneous results around 530°C for 18–20 kbar (Figure 12a). Interestingly, peak-metamorphic conditions retrieved for the main occurrences of the Cycladic Blueschists unit throughout the Aegean domain point to very similar maximum burial depths of ~ 60 km at *T* of ~ 500–550°C as retrieved on Tinos [*Parra et al*., 2002], Syros [*Trotet et al*., 2001a], Sifnos [*Trotet et al*., 2001b; *Schmädicke and Will*, 2003; *Groppo et al*., 2009], or Ios [e.g., *Huet*, 2010] using most of available thermobarometric methods. In addition, radiometric ages obtained on HP-LT rocks (eclogite and blueschist-facies rocks) show a relative synchronism within the narrow 50–40 Ma age range for peak-burial conditions (see recent synthesis of available age data in *Huet* [2010]). In the lights of these results, peak-burial conditions for the Cycladic Blueschists unit appear either quite similar or likely coeval. A first step of exhumation was then realized under a cold P/T gradient in the favor of layer-parallel décollement that allowed the preservation of the internal structure of the tectonics units. Therefore, just like in Oman, New Caledonia, or Corsica (France) [*Agard and Vitale-Brovarone*, 2013], burial and/or exhumation of continental material do not take place in corner flow or a mélange structures but in an accretionary structures that preserve the internal consistency of the metasediments or the nappe-stack architecture with higher-pressure conditions found in the lowermost units. These characteristics suggest that the lower Cycladic Blueschists subunit was detached at ~ 60 km depth from the downgoing plate probably toward the end of the subduction of the Pindos basin at circa 50–40 Ma. Having a clear continental affinity and supposed to represent the southern passive margin of the Pindos basin [e.g., *Jolivet et al*., 2004; *Jolivet and Brun*, 2010], the Cycladic Basement unit reached almost similar depths [*Huet*, 2010]. Based on the preservation of top-to-the-south thrust kinematics, in agreement with the large-scale reconstruction [*Huet et al*., 2009; *Jolivet and Brun*, 2010], it is proposed that detachment of the lower Cycladic Blueschists subunit from the subducting plate occurred as the result of the underplating of the more buoyant Cycladic Basement continental unit. This unit has then probably dragged the oceanic unit upward toward middle-to-upper crustal levels.

8.6. Implications for the Dynamics of the Aegean Back-Arc Domain

Historically, the first description of a large-scale extensional shear zone in the Aegean back-arc domain was the South Cyclades Shear Zone, exposed on Ios [*Lister et al*., 1984]. This pioneer result rapidly contrasted with the consistent well-constrained top-to-the-north deformation retrieved in the Northern Cyclades [*Faure and Bonneau*, 1988; *Faure et al*., 1991] and the Naxos MCC [*Gautier et al*., 1993; *Urai et al*., 1990; *Buick*, 1991] and more generally in most of the Northern and the Central Cyclades [*Gautier and Brun*, 1994a, 1994b]. Top-to-the-north deformation was even described in Ios and explained as a bivergent deformation

during exhumation [*Vandenberg and Lister*, 1996; *Forster and Lister*, 1999b; *Thomson et al*., 2009]. The complex deformation pattern visible on Ios was recently reinterpreted as the superimposition of two distinct tectonometamorphic events recognized in most parts of the Hellenic orogenic belt: (i) a synorogenic, Eocene top-to-the-south thrusting of the Cycladic Blueschists unit over the Cycladic Basement in a HP context coeval with a north dipping subduction followed by (ii) a postorogenic, Oligo-Miocene top-to-the-north deformation in the back-arc domain [*Huet et al*., 2009]. Postorogenic deformation, dominated by top-to-the-north extensional shear zones was viewed, at that stage, as strongly asymmetric [e.g., *Avigad and Garfunkel*, 1989, 1991; *Buick*, 1991; *Faure et al*., 1991; *Lee and Lister*, 1992; *Gautier et al*., 1993; *Gautier and Brun*, 1994a; *Jolivet and Patriat*, 1999; *Vanderhaeghe*, 2004; *Mehl et al*., 2005, 2007; *Denèle et al*., 2011]. More recently, these top-to-the-north extensional shear zones were all grouped in a single crustal-scale extensional structure known as the NCDS [*Jolivet et al*., 2010]. In parallel, coeval extensional shear zones were described in the Western Cyclades [*Grasemann and Petrakakis*, 2007; *Iglseder et al*., 2009, 2011; *Tschegg and Grasemann*, 2009; *Brichau et al*., 2010; *Schneider et al*., 2011] with top-to-the-south to -SW consistent kinematics and were recently grouped as the WCDS [*Grasemann et al*., 2012]. Extensional deformation in the Aegean back-arc domain is thus currently viewed as a rather symmetric or at least less noncoaxial. What is the impact of this study on this debate?

By studying a key yet weakly constrained segment of the Southern Cyclades, this study sheds new light on the long-standing debate about the symmetry or the asymmetry of the Aegean back-arc domain. While flanking the WCDS, Sikinos and Folegandros Islands are overwhelmingly dominated by a strong top-to-the-north asymmetry. Either the volume of the Cycladic Blueschists unit, the intra-Cycladic Blueschists shear zones or even the South Cycladic thrust that is therefore reactivated, all display conspicuously by top-to-the-north kinematics. Top-to-the-north, normal-sense motion over the intra-Cycladic Blueschists shear zones is strengthened by the repeated RSCM Tmax gaps. While absolute timing of top-to-the-north deformation still remains to be constrained, deformation is clearly recorded by synkinematic greenschist-facies recrystallizations that overprint the former HP imprint. A clear north-south strain continuum through the ductile-brittle transition is thus recorded with a persistence of the approximately north-south stretching as described on the Northern Cyclades [*Mehl et al*., 2005, 2007; *Denèle et al*., 2011]. Late exhumation stages in the brittle field are well constrained by low-temperature geochronology that appear either consistent with ongoing top-to-the-north shearing or coeval with the last deformation increments along the WCDS [e.g., *Brichau*, 2004; *Grasemann et al*., 2012]. By correlating the weak, brittle top-to-the-south deformation observed to the SW of Folegandros with the southeastern most termination of the WCDS, this study therefore bounds the area of influence of the WCDS. Deformation thus appears genuinely asymmetric in the center of the Aegean domain. Being the most prominent features of intense and localized extension of the continental crust, migmatite cored-MCC [*Rey et al*., 2009] or the a-type metamorphic domes [*Jolivet et al*., 2004] only occur in the center of the Aegean domain where deformation is highly asymmetric from Mykonos to the North, all the way to Sikinos to the South [e.g., *Gautier et al*., 1993; *Lucas*, 1999; *Kumerics et al*., 2005; *Denèle et al*., 2011]. Conversely, more marginal areas to the west and the east that connect to noncollapsed orogenic segments appear clearly less extended and are devoid of migmatite cored-MCC. There, symmetrically arranged detachment systems depict a more bivergent extensional system. In the western parts of the Aegean domain, both the WCDS and the NCDS act to exhume a horst-shaped central domain where synorogenic features are nicely preserved [e.g., *Grasemann et al*., 2012]. Similarly, rather symmetric patterns occur in the Eastern Cyclades and central Menderes region, to the east [*Hetzel et al*., 1995; *Gessner et al*., 2001; *Kumerics et al*., 2005]. A straightforward yet important correlation between the degree of noncoaxiality and the amount of stretching of the crust can then be proposed at the scale of the entire Aegean domain.

9. Conclusions

Sikinos and Folegandros Islands, located in a key yet poorly studied segment of the Aegean domain, have been studied to clarify the distribution of kinematic indicators in the Aegean Sea and to unambiguously separate deformation related to orogenic and postorogenic stages. By combining structural and petrological data, this study shows that the postorogenic deformation in the Southern Cyclades is extremely asymmetric as the whole structural succession of both the Cycladic Blueschists and the Cycladic Basement units is pervasively affected by top-to-the-north deformation. Top-to-the-north deformation exhibits series of strain gradients in the vicinity of four main intra-Cycladic Blueschists unit shear zones and the Cycladic Blueschists/Cycladic Basement contact operating in greenschist-facies conditions. Importance of the intra-Cycladic Blueschists unit

shear zones were retrieved using RSCM peak-metamorphic temperatures that showed a series of major normal-sense metamorphic gap describing an overall stepwise decrease of more than 200°C. The Cycladic Blueschists/Cycladic Basement contact and the Ambeli shear zone also recorded late increments of motions in brittle conditions with the development of thick cataclasite zones while the volume of both units experienced high-angle normal faulting. Inversion of fault slip data allows concluding that (1) kinematics of the ductile and the brittle structures present a marked consistency of the stretching direction indicating an approximately north-south strain continuum through the ductile-brittle transition and that (2) the high angle of the maximum principal stress axis to the detachments suggests a weak mechanical behavior of the damaged zone that allows motions at very shallow dip angle. While flanking the West Cycladic Detachment System, the Southern Cyclades are therefore overwhelmingly dominated by a strong top-to-the-north asymmetry during the postorogenic stages arguing for a genuinely asymmetric deformation in the center of the Aegean domain. Despite a strong top-to-the-north overprint in ductile and later brittle regimes and a partial retrogression in the greenschist-facies conditions, kinematics and metamorphic conditions that prevailed during the last steps of subduction were identified. Kinematics of the Cycladic Blueschists/Cycladic Basement contact, marked by an approximately 200 m thick top-to-the-north mylonitic and cataclastic zone appears clearly polyphased, with the preservation of initial top-to-the-south thrust kinematics inherited from the subduction zone. Peak-metamorphic conditions retrieved for the lower unit of the Cycladic Blueschists unit yielded typical approximately 18–20 kbar for 530°C, corresponding to peak-burial depths during the Pindos subduction. It is therefore proposed that, beyond the probable extrusion structure drawn for the Cycladic Blueschists accretionary structure, detachment of the lower Cycladic Blueschists subunit from the subducting plate occurred as the result of the underplating of the more buoyant Cycladic Basement continental unit.

Acknowledgments

All the data presented in this paper are available upon requests from the first author (R.A.); analytical techniques and a detailed description of outcrop conditions, mineral habits, phase relationships, and mineral compositions are given in the supporting information linked to the electronic version of this article. This study has been funded by the European Research Council (ERC) under the seventh Framework Programme of the European Union (ERC Advanced Grant, grant agreement 290864, RHEOLITH). Reviews by B. Grasemann and an anonymous referee helped in improving the manuscript. The authors are grateful to S. Janiec and J.G. Badin (ISTO) for the preparation of thin sections and I. Di Carlo (ISTO) for assistance during the numerous electron microprobe sessions.

References

Agard, P., and A. Vitale-Brovarone (2013), Thermal regime of continental subduction: The record from exhumed HP–LT terranes (New Caledonia, Oman, Corsica), *Tectonophysics*, *601*, 206–215.

Agard, P., R. Augier, and P. Monié (2011), Shear band formation and strain localization on a regional scale: Evidence from anisotropic rocks below a major detachment (Betic Cordilleras, Spain), *J. Struct. Geol.*, *33*(2), 114–131.

Andriessen, P. A. M., G. Banga, and E. H. Hebeda (1987), Isotopic age study of pre-Alpine rocks in the basal units on Naxos, Sikinos and Ios (Greek Cyclades), *Geol. Mijnbouw*, *66*, 3–14.

Angelier, J. (1976), Sur l'alternance mio-plio-quaternaire de mouvements extensifs et compressifs en Égée orientale: L'île de Samos (Grèce), *C. R. Acad. Sci., Ser. II*, *283*, 463–466.

Angelier, J. (1984), Tectonic analysis of fault slip data sets, *J. Geophys. Res.*, *89*(B7), 5835–5848, doi:10.1029/JB089iB07p05835.

Angelier, J. (1990), Inversion of field data in fault tectonics to obtain the regional stress: III. A new rapid direct inversion method by analytical means, *Geophys. J. Int.*, *103*, 363–376.

Angelier, J. (1994), Fault slip analysis and palaeostress reconstruction, in *Continental Deformation*, edited by P. L. Hancock, pp. 53–100, Elsevier, New York.

Angelier, J., G. Glaçon, and C. Muller (1978), Sur la présence et la position tectonique du Miocène inférieur marin dans l'archipel de Naxos (Cyclades, Grèce), *C. R. Acad. Sci., Ser. II*, *286*, 21–24.

Altherr, R., and W. Siebel (2002), I-type plutonism in a continental back-arc setting: Miocene granitoids and monzonites from the central Aegean Sea (Greece), *Contrib. Mineral. Petrol.*, *143*, 397–415.

Altherr, R., M. Schliestedt, M. Okrusch, E. Seidel, H. Kreuzer, W. Harre, H. Lenz, I. Wendt, and G. A. Wagner (1979), Geochronology of high-pressure rocks on Sifnos (Cyclades, Greece), *Contrib. Mineral. Petrol.*, *70*, 245–255.

Altherr, R., H. Kreuzer, I. Wendt, H. Lenz, G. A. Wagner, J. Keller, W. Harre, and A. Hohndorf (1982), A Late Oligocene/Early Miocene high temperature belt in the anti-cycladic crystalline complex (SE Pelagonian, Greece), *Geol. Jahrb.*, *23*, 97–164.

Angiboust, S., P. Agard, H. Raimbourg, P. Yamato, and B. Huet (2011), Subduction interface processes recorded by eclogite-facies shear zones (Monviso, W. Alps), *Lithos*, *127*(1), 222–238.

Aubouin, J., and J. Dercourt (1965), Sur la géologie de l'Egée: Regard sur la Crète (Grèce), *Bull. Soc. Geol. Fr.*, *7*, 787–821.

Augier, R., L. Jolivet, and C. Robin (2005a), Late Orogenic doming in the eastern Betic Cordilleras: Final exhumation of the Nevado-Filabride complex and its relation to basin genesis, *Tectonics*, *24*, TC4003, doi:10.1029/2004TC001687.

Augier, R., P. Agard, P. Monié, L. Jolivet, and C. Robin (2005b), Exhumation, doming and slab retreat in the Betic Cordillera (SE Spain): In situ $^{40}Ar/^{39}Ar$ ages and P-T-d-t paths for the Nevado-Filabride complex, *J. Metamorph. Geol.*, *23*, 357–381.

Augier, R., G. Booth-Rea, P. Agard, J. Martínez-Martínez, L. Jolivet, and J. Azañón (2005c), Exhumation constraints for the lower Nevado- Filabride Complex (Betic Cordillera, SE Spain): A Raman thermometry and Tweequ multiequilibrium thermobarometry approach, *Bull. Soc. Geol. Fr.*, *176*, 403–416.

Augier, R., L. Jolivet, D. Do coutoand, and F. Negro (2013), From ductile to brittle, late-to post-orogenic evolution of the Betic Cordillera: Structural insights from the northeastern Internal zones, *Bull. Soc. Geol. Fr.*, *184*(4–5), 405–425.

Avdis, V., and A. Photiades (1999), Sikinos and Folegandros geological map, scale 1:50,000, Institute of Geology and Mineral Exploration, Athens, Greece.

Avigad, D., and Z. Garfunkel (1989), Low-angle faults above and below a blueschist belt (Tinos Island, Cyclades, Greece), *Terra Nova*, *1*(2), 182–187.

Avigad, D., and Z. Garfunkel (1991), Uplift and exhumation of high-pressure metamorphic terrains: The example of the Cycladic blueschist belt (Aegean Sea), *Tectonophysics*, *188*(3), 357–372.

Avigad, D., A. Ziv, and Z. Garfunkel (2001), Ductile and brittle shortening, extension-parallel folds and maintenance of crustal thickness in the Central Aegean, *Tectonics*, *20*(2), 277–287, doi:10.1029/2000TC001190.

Baldwin, S. L. (1996), Contrasting P-T-t histories for blueschists from the western Baja Terrane and the Aegean; effects of synsubduction exhumation and backarc extension, in *Subduction: Top to Bottom*, edited by G. E. Bebout et al., pp. 135–141, AGU, Washington, D. C.

Baldwin, S. L., and G. S. Lister (1998), Thermochronology of the South Cyclades Shear Zone, Ios, Greece: Effects of ductile shear in the argon partial retention zone, *J. Geophys. Res.*, *103*, 7315–7336, doi:10.1029/97JB03106.

Bell, T. H., and M. J. Rubenach (1983), Sequential porphyroblast growth and crenulation cleavage development during progressive deformation, *Tectonophysics*, *92*(1), 171–194.

Beyssac, O., B. Goffe, C. Chopin, and J.-N. Rouzaud (2002), Raman spectra of carbonaceous material from metasediments: A new geothermometer, *J. Metamorph. Geol.*, *20*, 859–871.

Beyssac, O., F. Brunet, J. P. Petitet, B. Goffé, and J.-N. Rouzaud (2003), Experimental study of the microtextural and structural transformations of carbonaceous materials under pressure and temperature, *Eur. J. Mineral.*, *15*, 937–951.

Blake, M. C., M. Bonneau, J. Geyssant, J. R. Kienast, C. Lepvrier, H. Maluski, and D. Papanikolaou (1981), A geological reconnaissance of the Cyclacic blueschist belt (Greece), *Geol. Soc. Am. Bull.*, *92*, 247–254.

Bonneau, M. (1984), Correlation of the Hellenic nappes in the south-east Aegean and their tectonic reconstruction, in *The Geological Evolution of the Eastern Mediterranean*, edited by J. E. Dixon and A. H. F. Robertson, *Geol. Soc. London Spec. Publ.*, 517–527, Blackwell Scientific Publications, Oxford, U. K.

Bonneau, M., and J. R. Kienast (1982), Subduction, collision et schistes bleus: L'exemple de l'Egée (Grèce), *Bull. Soc. Geol. Fr.*, *24*, 785–791.

Bonneau, M., J. R. Kienast, C. Lepvrier, and H. Maluski (1980), Tectonique et métamorphisme haute pression d'âge Eocène dans les Hellénides: Exemple de l'île de Syros (Cyclades, Grèce), *C. R. Acad. Sci., Ser. II*, *291*, 171–174.

Bosse, V., M. Ballèvre, and O. Vidal (2002), Ductile thrusting recorded by the garnet isograd from blueschist-facies metapelites of the Ile de Groix (Armorican Massif, France), *J. Petrol.*, *43*(3), 485–510.

Bozkurt, E. (2003), Origin of NE-trending basins in Western Turkey, *Geodinamica Acta*, *16*, 61–81.

Bozkurt, E., and R. G. Park (1997), Evolution of a mid-Tertiary extensional shear zone in the Southern Menderes Massif, western Turkey, *Bull. Soc. Geol. Fr.*, *168*, 3–14.

Brichau, S. (2004), Constraining the tectonic evolution of extensional fault systems in the Cyclades (Greece) using low-temperature themochronology, PhD thesis, 345 pp., Univ. of Montpelier II, Montpelier, France.

Brichau, S., S. Thomson, and U. Ring (2010), Thermochronometric constraints on the tectonic evolution of the Serifos detachment (Aegean Sea, Greece), *Int. J. Earth Sci.*, *99*, 379–393, doi:10.1007/s00531-008-0386-0.

Bröcker, M. (1990), Blueschist-to-greenschist transition in metabasites from Tinos Island, Cyclade, Greece: Compositional control or fluid infiltration, *Lithos*, *25*, 25–39, doi:10.1016/0024-4937(90)90004-K.

Bröcker, M., and L. Franz (1998), Rb-Sr isotope studies on Tinos Island (Cyclades, Greece): Additional time constraints for metamorphism, extent of infiltration-controlled overprinting and deformational activity, *Geol. Mag.*, *135*, 369–382, doi:10.1017/S0016756898008681.

Bröcker, M., and R. T. Pidgeon (2007), Protolith ages of meta-igneous and metatuffaceous rocks from the Cycladic Blueschist Unit (Greece): Results of a reconnaissance U–Pb Zircon study, *J. Geol.*, *115*, 83–98.

Brunn, J. H., I. Argyriadis, L. E. Ricou, A. Poisson, J. Marcoux, and P. C. de Graciansky (1976), Eléments majeurs de liaison entre Taurides et Hellénides, *Bull. Soc. Geol. Fr.*, *18*, 481–497.

Bolhar, R., U. Ring, and C. M. Allen (2010), An integrated zircon geochronological and geochemical investigation into the Miocene plutonic evolution of the Cyclades, Aegean Sea, Greece: Part 1: Geochronology, *Contrib. Mineral. Petrol.*, *160*(5), 719–742.

Buick, I. S. (1988), The metamorphic and structural evolution of the Barrovian overprint, Naxos, Cyclades, Greece, PhD thesis, 235 pp., Univ. of Cambridge, Cambridge, U. K.

Buick, I. S. (1991), The late alpine evolution of an extensional shear zone (Naxos, Greece), *J. Geol. Soc. London*, *148*, 93–103, doi:10.1144/gsjgs.148.1.0093.

Buick, I. S., and T. J. B. Holland (1989), The P-T-t path associated with crustal extension, Naxos (Cyclades, Greece), in *Evolution of Metamorphic Belts*, edited by J. S. Daly, *Geol. Soc. London Spec. Publ.*, *43*, 365–369.

Denèle, Y., E. Lecomte, L. Jolivet, O. Lacombe, L. Labrousse, B. Huet, and L. Le Pourhiet (2011), Granite intrusion in a metamorphic core complex: The example of the Mykonos laccolith (Cyclades, Greece), *Tectonophysics*, *501*(1), 52–70.

Dewey, J. F. (1988), Extensional collapse of orogens, *Tectonics*, *7*, 1123–1139, doi:10.1029/TC007i006p01123.

Duchêne, S., R. Aïssa, and O. Vanderhaeghe (2006), Pressure-temperature-time evolution of metamorphic rocks from Naxos (Cyclades, Greece): Constraints from thermobarometry and Rb/Sr dating, *Geodyn. Acta*, *19*, 30–321, doi:10.3166/ga.19.301-321.

Dürr, S., E. Seidel, H. Kreuzer, and W. Harre (1978), Témoins d'un métamorphisme d'âge crétacé supérieur dans l'Egeide: Datations radiométriques de minéraux provenant de l'île de Nikouria (Cyclades, Grèce), *Bull. Soc. Geol. Fr.*, *20*, 209–213.

Eskola, P. (1920), Om metasomatiska omvandlingar i silikatbergarter, *Norsk Geol.*, *6*, 89–108.

Faccenna, C., C. Piromallo, A. Crespo-Blanc, L. Jolivet, and F. Rossetti (2004), Lateral slab deformation and the origin of the western Mediterranean arcs, *Tectonics*, *23*, TC1012, doi:10.1029/2002TC001488.

Faccenna, C., A. Heuret, F. Funiccello, S. Lallemand, and T. W. Becker (2007), Predicting trench and plate motion from the dynamics of a strong slab, *Earth Planet. Sci. Lett.*, *257*, 29–36.

Faure, M., and M. Bonneau (1988), Données nouvelles sur l'extension néogène de l'Egée: La déformation ductile du granite miocène de Mykonos (Cyclades, Grèce), *C. R. Acad. Sci., Ser. II*, *307*(13), 1553–1559.

Faure, M., M. Bonneau, and J. Pons (1991), Ductile deformation and syntectonic granite emplacement during the late Miocene extension of the Aegean (Greece), *Bull. Soc. Geol. Fr.*, *162*, 3–12.

Franz, L., M. Okrusch, and M. Bröcker (1993), Polymetamorphic evolution of the pre-Alpidic basement rocks on the island of Sikinos (Cyclades, Greece), *Neues Jahrb. Mineral. Monatsh.*, *4*, 145–162.

Forster, M. A., and G. S. Lister (1999a), Detachment faults in the Aegean core complex of Ios, Cyclades, Greece, in *Exhumation Processes: Normal Faulting, Ductile Flow and Erosion*, edited by U. Ring et al., *Geol. Soc. London Spec. Publ.*, *154*, 305–323.

Forster, M. A., and G. S. Lister (1999b), Separate episodes of eclogite and blueschist-facies metamorphism in the Aegean metamorphic core complex of Ios (Cyclades, Greece), *Continental Tectonics*, edited by C. Mac Niocall and P. D. Ryan, *Geol. Soc. London Spec. Publ.*, *164*, 157–177.

García-Dueñas, V., J. Balanya, and J. Martínez-Martínez (1992), Miocene extensional detachments in the outcropping basement of the northern Alboran basin (Betics) and their tectonic implications, *Geo Mar. Lett.*, *12*, 88–95.

Gautier, P., and J. P. Brun (1994a), Crustal-scale geometry and kinematics of late-orogenic extension in the central Aegean (Cyclades and Evvia Island), *Tectonophysics*, *238*, 399–424, doi:10.1016/0040-1951(94)90066-3.

Gautier, P., and J. P. Brun (1994b), Ductile crust exhumation and extensional detachments in the central Aegean (Cyclades and Evvia islands), *Geodinamica Acta*, *7*, 57–85.

Gautier, P., J. P. Brun, and L. Jolivet (1993), Structure and kinematics of upper Cenozoic extensional detachement on Naxos and Paros (Cyclades Islands, Greece), *Tectonics*, *12*, 1180–1194, doi:10.1029/93TC01131.
Gessner, K., U. Ring, C. Johnson, R. Hetzel, C. W. Passchier, and T. Güngör (2001), An active bivergent rolling-hinge detachment system: Central Menderes metamorphic core complex in western Turkey, *Geology*, *29*(7), 611–614.
Goscombe, B. D., C. W. Passchier, and M. Hand (2004), Boudinage classification: End-member boudin types and modified boudin structures, *J. Struct. Geol.*, *26*(4), 739–763.
Grasemann, B., and P. Petrakakis (2007), Evolution of the Serifos Metamorphic Core Complex, *J. Virtual Explorer*, *27*, doi:10.3809/jvir-tex.2007.00170.
Grasemann, B., S. Martel, and C. Passchier (2005), Reverse and normal drag along a fault, *J. Struct. Geol.*, *27*, 999–1010, doi:10.1016/j.jsg.2005.04.006.
Grasemann, B., D. A. Schneider, D. F. Stöckli, and C. Iglseder (2012), Miocene bivergent crustal extension in the Aegean: Evidence from the western Cyclades (Greece), *Lithosphere*, *4*(1), 23–39.
Groppo, C., M. Forster, G. Lister, and R. Compagnoni (2009), Glaucophane schists and associated rocks from Sifnos (Cyclades, Greece): New constraints on the P–T evolution from oxidized systems, *Lithos*, *109*(3), 254–273.
Gueydan, F., Y. M. Leroy, L. Jolivet, and P. Agard (2003), Analysis of continental midcrustal strain localization induced by microfracturing and reaction-softening, *J. Geophys. Res.*, *108*(B2), 2064, doi:10.1029/2001JB000611.
Gupta, S. (1995), Structure and metamorphism of Sikinos, Cyclades, Greece, PhD thesis, 248 pp., Univ. of Cambridge, Cambridge, U. K.
Gupta, S., and M. J. Bickle (2004), Ductile shearing, hydrous fluid channelling and high-pressure metamorphism along the basement-cover contact on Sikinos, Cyclades, Greece, in *Flow Processes in Faults and Shear Zones*, edited by G. I. Alsop, et al., *Geol. Soc. London Spec. Publ.*, *224*, 161–175, doi:10.1144/GSL.SP.2004.224.01.11.
Hancock, P. L. (1985), Brittle microtectonics: Principles and practice, *J. Struct. Geol.*, *7*(3–4), 437–457.
Henjes-Kunst, F., and H. Kreuzer (1982), Isotopic dating of pre-alpidic rocks from the Island of Ios (Cyclades,Greece), *Contrib. Mineral. Petrol.*, *80*, 245–253, doi:10.1007/BF00371354.
Hetzel, R., C. W. Passchier, U. Ring, and Ö. O. Dora (1995), Bivergent extension in orogenic belts: The Menderes massif (southwestern Turkey), *Geology*, *23*(5), 455–458.
Holland, T. J. B., and R. Powell (1998), An internally consistent thermodynamic data set for phases of petrological interest, *J. Metamorph. Geol.*, *16*(3), 309–343.
Huet, B. (2010), Rhéologie de la lithosphère continentale: L'exemple de la Mer Egée, PhD thesis, 402 pp., Univ. of Pierre et Marie Curie-Paris VI, Paris, France.
Huet, B., L. Labrousse, and L. Jolivet (2009), Thrust or detachment? Exhumation processes in the Aegean: Insight from a field study on Ios (Cyclades, Greece), *Tectonics*, *28*, TC3007, doi:10.1029/2008TC002397.
Huet, B., L. Le Pourhiet, L. Labrousse, E. Burov, and L. Jolivet (2011), Post-orogenic extension and metamorphic core complexes in a heterogeneous crust: The role of crustal layering inherited from collision: Application to the Cyclades (Aegean domain), *Geophys. J. Int.*, *184*(2), 611–625.
Iglseder, C., B. Grasemann, D. A. Schneider, K. Petrakakis, C. Miller, U. S. Klötzli, M. Thöni, A. Zámolyi, and C. Rambousek (2009), I- and S-type plutonism on Serifos (W-Cyclades, Greece), *Tectonophysics*, *473*, 69–83, doi:10.1016/j.tecto.2008.09.021.
Iglseder, C., B. Grasemann, A. H. N. Rice, K. Petrakakis, and D. A. Schneider (2011), Miocene south directed low-angle normal fault evolution on Kea Island (West Cycladic Detachment System, Greece), *Tectonics*, *30*, TC4013, doi:10.1029/2010TC002802.
Jabaloy, A., J. Galindo-Zaldívar, and J. González-Lodeiro (1993), The Alpujarride-Nevado-Filabride extensional shear zone (Betic Cordillera, SE Spain), *J. Struct. Geol.*, *15*, 555–569, doi:10.1016/0191-8141(93)90148-4.
Jacobshagen, V. (1986), Geologie von Griechland, PhD thesis, 279 pp., Univ. of Borntraeger, Berlin-Stuttgart, Germany.
Jacobshagen, V., S. Dürr, F. Kockel, K. O. Kopp, G. Kowalczyk, H. Berckhemer, and D. Büttner (1978), Structure and geodynamic evolution of the Aegean region, in *Alps, Apennines and Hellenides*, edited by H. Cloos et al., pp. 537–564, International Union of Geodesy and Geophysics, Stuttgart, Germany.
Jansen, J. B. H. (1973), Naxos geological map, scale 1:50,000, Institute of Geology and Mineral Exploration, Athens.
Jansen, J. B. H. (1977), Metamorphism on Naxos, Greece, PhD thesis, 237 pp., Univ. of Utrecht, Utrecht, Netherlands.
Jansen, J. B. H., and R. D. Schuiling (1976), Metamorphism on Naxos: Petrology and geothermal gradients, *Am. J. Sci.*, *276*, 1225–1253.
Jolivet, L., and J. P. Brun (2010), Cenozoic geodynamic evolution of the Aegean, *Int. J. Earth Sci.*, *99*, 109–138, doi:10.1007/s00531-008-0366-4.
Jolivet, L., and C. Faccenna (2000), Mediterranean extension and the Africa-Eurasia collision, *Tectonics*, *19*(6), 1095–1106, doi:10.1029/2000TC900018.
Jolivet, L., and M. Patriat (1999), Ductile extension and the formation of the Aegean Sea, in *The Mediterranean Basins: Tertiary Extension Within the Alpine Orogen*, edited by B. Durand et al., *Geol. Soc. London Spec. Publ.*, 427–456.
Jolivet, L., J. P. Brun, P. Gautier, S. Lallemand, and M. Patriat (1994), 3-D kinematics of extension in the Aegean from the Early Miocene to the present, insight from the ductile crust, *Bull. Soc. Geol. Fr.*, *165*, 195–209.
Jolivet, L., C. Faccenna, B. Goffé, M. Mattei, F. Rossetti, C. Brunet, and T. Parra (1998), Midcrustal shear zones in postorogenic extension: Example from the northern Tyrrhenian Sea, *J. Geophys. Res.*, *103*(B6), 12,123–12,160, doi:10.1029/97JB03616.
Jolivet, L. C., B. G. Faccenna, E. Burov, and P. Agard (2003), Subduction tectonics and exhumation of high-pressure metamorphic rocks in the Mediterranean orogens, *Am. J. Sci.*, *303*, 353–409, doi:10.2475/ajs.303.5.353.
Jolivet, L., V. Famin, C. Mehl, T. Parra, C. Aubourg, R. Hébert, and P. Philippot (2004), Progressive strain localisation, boudinage and extensional metamorphic complexes, the Aegean Sea case, in *Gneiss Domes in Orogeny*, 380, edited by D. L. Whitney, C. Teyssier, and C. S. Siddoway, *Geol. Soc. London Spec. Pap., 380*.,185–210, Boulder, Colo.
Jolivet, L., R. Augier, C. Faccenna, F. Negro, G. Rimmele, P. Agard, C. Robin, F. Rossetti, and A. Crespo-Blanc (2008), Subduction, convergence and the mode of back-arc extension in the Mediterranean region, *Bull. Soc. Geol. Fr.*, *179*, 525–550, doi:10.2113/gssgfbull.179.6.525.
Jolivet, L., E. Lecomte, B. Huet, Y. Denèle, O. Lacombe, L. Labrousse, L. Le Pourhiet, and C. Mehl (2010), The North Cycladic detachment system, *Earth Planet. Sci. Lett.*, *289*, 87–104, doi:10.1016/j.epsl.2009.10.032.
Katzir, Y., A. Matthews, Z. Garfunkel, M. Schliestedt, and D. Avigad (1996), The tectono-metamorphic evolution of a dismembered ophiolite (Tinos, Cyclades, Greece), *Geol. Mag.*, *133*, 237–254.
Katzir, Y., D. Avigad, A. Matthews, Z. Garfunkel, and B. W. Evans (1999), Origin and metamorphism of ultrabasic rocks associated with a subducted continental margin, Naxos (Cyclades, Greece), *J. Metamorph. Geol.*, *17*, 301–318.
Keay, S. (1998), The geological evolution of the Cyclades, Greece, constraints from SHRIMP U/Pb geochronology, PhD thesis, 317pp., Research School of Earth Sciences, Australian National Univ., Camberra, Australia.
Keay, S., and G. S. Lister (2002), African provenance for the metasediments and metaigneous rocks of the Cyclades, Aegean Sea, Greece, *Geology*, *30*(3), 235–238.

Keay, S., G. S. Lister, and I. Buick (2001), The timing of partial melting, Barrovian metamorphism and granite intrusion in the Naxos metamorphic core complex, Cyclades, Aegean Sea, Greece, *Tectonophysics*, *342*, 275–312.
Keiter, M., K. Piepjohn, C. Ballhaus, M. Lagos, and M. Bode (2004), Structural development of high-pressure metamorphic rocks on Syros island (Cyclades, Greece), *J. Struct. Geol.*, *26*, 1433–1445.
Krohe, A., E. Mposkos, A. Diamantopoulos, and G. Kaouras (2010), Formation of basins and mountain ranges in Attica (Greece): The role of Miocene to Recent low-angle normal detachment faults, *Earth Sci. Rev.*, *98*, 81–104, doi:10.1016/j.earscirev.2009.10.005.
Kuhlemann, J., W. Frisch, I. Dunkl, M. Kázmér, and G. Schmiedl (2004), Miocene siliciclastic deposits of Naxos Island: Geodynamic and environmental implications for the evolution of the southern Aegean Sea (Greece), in *Detrital Thermochronology, Provenance Analysis, Exhumation, and Landscape Evolution of Mountain Belts*, *Geol. Soc. Am. Spec. Pap.*, edited by M. Bernet and C. Spiegel, pp. 51–65, Geol. Soc. of Am., Boulder, Colo.
Kumerics, C., U. Ring, S. Brichau, J. Glodny, and P. Monié (2005), The extensional Messaria shear zone and associated brittle detachment faults (Aegean Sea, Greece), *J. Geol. Soc.*, *162*(4), 701–721.
Lahfid, A., O. Beyssac, E. Deville, F. Negro, C. Chopin, and B. Goffé (2010), Evolution of the Raman spectrum of carbonaceous material in low-grade metasediments of the Glarus Alps (Switzerland), *Terra Nova*, *22*(5), 354–360.
Lecomte, E., L. Jolivet, O. Lacombe, Y. Denèle, L. Labrousse, and L. Le Pourhiet (2010), Geometry and kinematics of Mykonos detachment, Cyclades, Greece: Evidence for slip at shallow dip, *Tectonics*, *29*, TC5012, doi:10.1029/2009TC002564.
Lee, J., and G. S. Lister (1992), Late Miocene ductile extension and detachment faulting (Mykonos, Greece), *Geology*, *20*, 121–124.
Le Pichon, X. (1982), Land-locked oceanic basins and continental collision, the eastern Mediterranean as a case example, in *Mountain Building Processes*, edited by K. J. Hsue, pp. 201–211, Academic Press, London.
Le Pichon, X., and J. Angelier (1981), The Aegean Sea, *Philos. Trans. R. Soc. London*, *300*, 357–372.
Lister, G. S., G. Banga, and A. Feenstra (1984), Metamorphic core complexes of cordilleran type in the Cyclades (Aegean Sea, Greece), *Geology*, *12*, 221–225, doi:10.1130/0091-7613(1984)12<221.
Lucas, I. (1999), Le pluton de Mykonos-Delos-Rhenee (Cyclades, Grèce): Un exemple de mise en place synchrone de l'extension crustale, PhD thesis, 319 pp., Univ. of Orléans, Orléans, France.
Malinverno, A., and W. Ryan (1986), Extension in the Tyrrhenian Sea and shortening in the Apennines as result of arc migration driven by sinking of the lithosphere, *Tectonics*, *5*, 227–245, doi:10.1029/TC005i002p00227.
Maluski, H., M. Bonneau, and J. R. Kienast (1987), Dating the metamorphic events in the Cycladic area: $^{39}Ar/^{40}Ar$ data from metamorphic rocks of the island of Syros (Greece), *Bull. Soc. Geol. Fr.*, *8*, 833–842.
Martin, L., S. Duchêne, E. Deloule, and O. Vanderhaeghe (2006), The isotopic composition of zircon and garnet: A record of the metamorphic history of Naxos, Greece, *Lithos*, *87*(3), 174–192.
Martínez-Martínez, J. M., J. I. Soto, and J. C. Balanya (2004), Elongated domes in extended orogens: A mode of mountain uplift in the Betics (Southeast Spain), in *Gneiss Domes in Orogeny*, vol. 380, edited by D. L. Whitney, C. Teyssier, and C. S. Siddoway, pp. 243–266, Geol. Soc. of Am., Boulder, Colo.
Mehl, C., L. Jolivet, and O. Lacombe (2005), From ductile to brittle: Evolution and localization of deformation below a crustal detachment (Tinos, Cyclades, Greece), *Tectonics*, *24*, TC4017, doi:10.1029/2004TC001767.
Mehl, C., L. Jolivet, O. Lacombe, L. Labrousse, and G. Rimmelé (2007), Structural evolution of Andros island (Cyclades, Greece): A key to the behaviour of a flat detachment within an extending continental crust, in *The Geodynamics of the Aegean and Anatolia*, edited by T. Taymaz, Y. Dilek, and Y. Ylmaz, *Geol. Soc. London Spec. Publ.*, 41–73, doi:10.1144/SP291.30305-8719/07.
Menant, A., L. Jolivet, R. Augier, and N. Skarpelis (2013), The North Cycladic Detachment System and associated mineralization, Mykonos, Greece: Insights on the evolution of the Aegean domain, *Tectonics*, *32*, 433–452, doi:10.1002/tect.20037.
Papanikolaou, D. (1987), Tectonic evolution of the Cycladic blueschist belt (Aegean Sea, Greece), in *Chemical Transport in Metasomatic Processes*, edited by H. C. Helgeson, pp. 429–450, D. Reidel, Dordrecht, Germany.
Parra, T., O. Vidal, and L. Jolivet (2002), Relation between deformation and retrogression in blueschist metapelites of Tinos island (Greece) evidenced by chlorite-mica local equilibria, *Lithos*, *63*, 41–66.
Passchier, C. W., and C. Simpson (1986), Porphyroclast systems as kinematic indicators, *J. Struct. Geol.*, *8*(8), 831–843.
Patriat, M., and L. Jolivet (1998), Post-orogenic extension and shallow-dipping shear zones, study of a brecciated decollement horizon in Tinos (Cyclades, Greece), *C. R. Acad. Sci., Ser. II*, *326*, 355–362.
Patzak, M., M. Okrusch, and H. Kreuzer (1994), The Akrotiri Unit of the island of Tinos, Cyclades, Greece: Witness to a lost terrane of Late Cretaceous age, *Neues Jahrb. Mineral. Abh.*, *194*, 211–252.
Photiades, A., and S. Keay (2003), Geological and geochronological data for Sikinos and Folegandros metamorphic units (Cyclades, Greece): Their tectono-stratigraphic significance, *Bull. Geol. Soc. Greece*, *35*, 35–45.
Platt, J. P., and R. L. M. Vissers (1989), Extensional collapse of thickened continental lithosphere: A working hypothesis for the Alboran Sea and Gibraltar arc, *Geology*, *17*, 540–543.
Plunder, A., P. Agard, B. Dubacq, C. Chopin, and M. Bellanger (2012), How continuous and precise is the record of P–T paths? Insights from combined thermobarometry and thermodynamic modelling into subduction dynamics (Schistes-Lustrés, W. Alps), *J. Metamorph. Geol.*, *30*(3), 323–346.
Powell, R., and T. J. B. Holland (1994), Optimal geothermometry and geobarometry, *Am. Mineral.*, *79*, 120–133.
Reinecke, T., R. Altherr, B. Hartung, K. Hatzipanagiotou, H. Kreuzer, W. Harre, H. Klein, J. Keller, E. Geenen, and H. Böger (1982), Remnants of a Late Cretaceous high temperature bet on the island of Anafi (Cyclades, Greece), *Neues Jahrb. Mineral. Abh.*, *145*, 157–182.
Rey, P. F., C. Teyssier, and D. L. Whitney (2009), The role of partial melting and extensional strain rates in the development of metamorphic core complexes, *Tectonophysics*, *477*(3), 135–144.
Ring, U., S. Laws, and M. Bernet (1999), Structural analysis of a complex nappe sequence and late-orogenic basins from the Aegean Island of Samos, Greece, *J. Struct. Geol.*, *21*, 1575–1601.
Ring, U., J. Glodny, T. Will, and S. Thomson (2007a), An Oligocene extrusion wedge of blueschist-facies nappes on Evia, Aegean Sea, Greece: Implications for the early exhumation of high-pressure rocks, *J. Geol. Soc.*, *164*, 637–652.
Ring, U., T. Will, J. Glodny, C. Kumerics, K. Gessner, S. Thomson, T. Güngör, P. Monié, M. Okrusch, and K. Drüppel (2007b), Early exhumation of high-pressure rocks in extrusion wedges: Cycladic blueschist unit in the eastern Aegean, Greece, and Turkey, *Tectonics*, *26*, TC2001, doi:10.1029/2005TC001872.
Ring, U., J. Glodny, T. Will, and S. Thomson (2010), The Hellenic subduction system: High-pressure metamorphism, exhumation, normal faulting, and large-scale extension, *Annu. Rev. Earth Planet. Sci.*, *38*, 45–76, doi:10.1146/annurev.earth.050708.170910.
Ring, U., J. Glodny, T. Will, and S. Thomson (2011), Normal faulting on Sifnos and the South Cycladic detachment system (Aegean Sea, Greece), *J. Geol. Soc.*, *168*, 751–768, doi:10.1144/0016-76492010-064.

Rosendaum, G., G. S. Lister, and C. Duboz (2002), Relative motion of Africa, Iberia and Europe during Alpine orogeny, *Tectonophysics*, *359*, 117–129.
Rossetti, F., C. Faccenna, L. Jolivet, F. Tecce, R. Funiciello, and C. Brunet (1999), Syn- versus post-orogenic extension in the Tyrrhenian Sea, the case study of Giglio Island (northern Tyrrhenian Sea, Italy), *Tectonophysics*, *304*, 71–93, doi:10.1016/S0040-1951(98)00304-7.
Royden, L. H. (1993), Evolution of retreating subduction boundaries formed during continental collision, *Tectonics*, *12*(3), 629–638, doi:10.1029/92TC02641.
Sánchez-Gómez, M., D. Avigad, and A. Heimann (2002), Geochronology of clasts in allochthonous Miocene sedimentary sequences on Mykonos and Paros Islands: Implications for back-arc extension in the Aegean Sea, *J. Geol. Soc.*, *159*, 45–60, doi:10.1144/0016-764901031.
Schliestedt, M., R. Altherr, and A. Mattews (1987), Evolution of the Cycladic crystalline complex: Petrology, isotope geochemistry and geochronology, in *Chemical Transport in Metasomatic Processes*, edited by H. C. Helgerson, pp. 389–428, D. Reidel, Dordrecht, Netherlands.
Schmädicke, E., and T. M. Will (2003), Pressure–temperature evolution of blueschist-facies rocks from Sifnos, Greece, and implications for the exhumation of high-pressure rocks in the Central Aegean, *J. Metamorph. Geol.*, *21*(8), 799–811.
Schneider, D. A., C. Senkowski, H. Vogel, B. Grasemann, C. Iglseder, and A. K. Schmitt (2011), Eocene tectonometamorphism on Serifos (western Cyclades) deduced from zircon depth-profiling geochronology and mica thermochronology, *Lithos*, *125*, 151–172, doi:10.1016/j.lithos.2011.02.005.
Schumacher, J. C., J. B. Brady, J. T. Cheney, and R. R. Tonnsen (2008), Glaucophane-bearing marbles on Syros (Greece), *J. Petrol.*, *49*(9), 1667–1686.
Spakman, W., and R. Wortel (2004), A tomographic view on western Mediterranean geodynamics, in *The TRANSMED Atlas. The Mediterranean Region From Crust to Mantle*, edited by F. Cavazza et al., pp. 31–52, Springer, Heidelberg, Germany.
Spear, F. S. (1993), Metamorphic phase equilibria and pressure-temperature-time path, in *Mineralogical Society of America Monograph*, edited by P. H. Ribbe, 789, pp., Mineralogical Soc. of Am., Washington, D. C.
Spear, F. S., D. D. Hickmott, and J. Selverstone (1990), Metamorphic consequences of thrust emplacement (Fall Mountain, New Hampshire), *Geol. Soc. Am.*, *102*, 1344–1360.
Sowa, A. (1985), Die Geologie der Insel Folegandros (Kykladen, Griechenland), *Erlangen Geol. Abh.*, *112*, 85–101.
Sternai, P., L. Jolivet, A. Menant, and T. Gerya (2014), Driving the upper plate surface deformation by slab rollback and mantle flow, *Earth Planet. Sci. Lett.*, *405*, 110–118, doi:10.1116/j.epsl.2014.08.023.
Thomson, S. N., U. Ring, S. Brichau, J. Glodny, and T. M. Will (2009), Timing and nature of formation of the Ios metamorphic core complex, southern Cyclades (Greece), in *Extending a Continent: Architecture, Rheology and Heat Budget*, edited by U. Ring and B. Wernicke, *Geol. Soc. London Spec Publ.*, *321*, 139–167.
Trotet, F., L. Jolivet, and O. Vidal (2001a), Tectono-metamorphic evolution of Syros and Sifnos Islands (Cyclades, Greece), *Tectonophysics*, *338*, 179–206.
Trotet, F., O. Vidal, and L. Jolivet (2001b), Exhumation of Syros and Sifnos metamorphic rocks (Cyclades, Greece): New constraints on the P–T paths, *Eur. J. Mineral.*, *13*, 901–920.
Tschegg, C., and B. Grasemann (2009), Deformation and alteration of a granodiorite during low-angle normal faulting (Serifos, Greece), *Lithosphere*, *1*, 139–154, doi:10.1130/L33.1.
Urai, J. L., R. D. Schuiling, and J. B. H. Jansen (1990), Alpine deformation on Naxos (Greece), *Geol. Soc. London Spec. Publ.*, *54*(1), 509–522.
Vandenberg, L. C., and G. S. Lister (1996), Structural analysis of basement tectonics from the Aegean metamorphic core complex of Ios, Cyclades, Greece, *J. Struct. Geol.*, *18*, 1437–1454, doi:10.1016/S0191-8141(96)00068-5.
van der Maar, P. A. (1980), The geology and petrology of Ios (Cyclades, Greece), *Ann. Geol. Pays Hell.*, *30*, 206–224.
van der Maar, P. A., B. W. Vink, and B. H. Jansen (1981), Ios geological map, scale 1:50,000, Institute of Geology and Mineral Exploration, Athens, Greece.
van der Maar, P. A., and J. B. H. Jansen (1983), The geology of the polymetamorphic complex of Ios, Cyclades, Greece and its significance for the Cycladic Massif, *Geol. Rundsch.*, *72*, 283–299, doi:10.1007/BF01765910.
Vanderhaeghe, O. (2004), Structural development of the Naxos migmatite dome, in *Gneiss Domes in Orogeny*, *Geol. Soc. Am. Spec. Pap.*, vol. 380, edited by D. L. Whitney, C. Teyssier, and C. S. Siddoway, pp. 211–227, Boulder, Colo.
van Hinsbergen, D. J. J., C. G. Langereis, and J. E. Meulenkamp (2005), Revision of timing, magnitude and distribution of Neogene rotations in the western Aegean region, *Tectonophysics*, *396*, 1–34, doi:10.1016/j.tecto.2004.10.001.
Wei, C., and R. Powell (2004), Calculated phase relations in high-pressure metapelites in the system NKFMASH (Na_2O–K_2O–FeO–MgO–Al_2O_3–SiO_2–H_2O), *J. Petrol.*, *45*(1), 183–202.
Weidmann, M., N. Solounias, R. E. Drake, and G. H. Curtis (1984), Neogene stratigraphy of the eastern basin, Samos island, Greece, *Geobios*, *17*(4), 477–490.
Whitney, D. L., and B. W. Evans (2010), Abbreviations for names of rock-forming minerals, *Am. Mineral.*, *95*(1), 185–186.
Wortel, M. J. R., and W. Spakman (2000), Subduction and slab detachment in the Mediterranean-Carpathian region, *Science*, *290*, 1910–1917.
Wijbrans, J. R., and I. McDougall (1986), $^{40}Ar/^{39}Ar$ dating of white micas from an alpine high-pressure metamorphic belt on Naxos (Greece): The resetting of the argon isotopic system, *Contrib. Mineral. Petrol.*, *93*, 187–194, doi:10.1007/BF00371320.